**Atmospheric
Chemistry
and Physics
Discussions**

Photochemistry of
VOCs and halogens
in the MBL

K. Toyota et al.

Title Page

Abstract	Introduction
Conclusions	References
Tables	Figures

|◄ | ►|

◄ | ►

Back | Close

Full Screen / Esc

Print Version

Interactive Discussion

© EGU 2003

A box model study on photochemical interactions between VOCs and reactive halogen species in the marine boundary layer

K. Toyota[1], Y. Kanaya[1], M. Takahashi[1, 2], and H. Akimoto[1]

[1]Frontier Research System for Global Change, Yokohama, Japan
[2]Also at Center for Climate System Research, The University of Tokyo, Tokyo, Japan

Correspondence to: K. Toyota (toyota@jamstec.go.jp)

Abstract

A new chemical scheme is developed for the multiphase photochemical box model SEAMAC (size-SEgregated Aerosol model for Marine Air Chemistry) to investigate photochemical interactions between volatile organic compounds (VOCs) and reactive halogen species in the marine boundary layer (MBL). Based primarily on critically eval-
5 uated kinetic and photochemical rate parameters as well as a protocol for chemical mechanism development, the new scheme has achieved a near-explicit treatment of oxidative degradation of up to C_3-hydrocarbons (CH_4, C_2H_6, C_3H_8, C_2H_4, C_3H_6, and C_2H_2) initiated by reactions with OH radicals, Cl- and Br-atoms, and O_3. Rate con-
10 stants and product yields for reactions involving halogen species are taken from the literature where available, but the majority of them need to be estimated. In partic- ular, addition reactions of halogen atoms with alkenes will result in the formation of halogenated organic intermediates, whose photochemical loss rates are carefully eval- uated in the present work. Model calculations with the new chemical scheme reveal
15 that the oceanic emissions of acetaldehyde (CH_3CHO) and alkenes (especially C_3H_6) are important factors for regulating reactive halogen chemistry in the MBL by promot- ing the conversion of Br atoms into HBr or more stable brominated intermediates in the organic form. The latter include brominated hydroperoxides, bromoacetaldehyde, and bromoacetone, which sequester bromine from reactive inorganic pool. The total mixing
20 ratio of brominated organic species thus produced is likely to reach 10–20% or more of that of inorganic gaseous bromine species over wide regions over the ocean. On the other hand, the reaction between Br atoms and C_2H_2 is unimportant for determining the degree of bromine activation in the remote MBL. It is suggested that peroxyacetic acid formed via CH_3CHO oxidation is one of the important chemical agents for triggering
25 autocatalytic halogen release from sea-salt aerosols. These results imply that reactive halogen chemistry can mediate a link between the oceanic emissions of VOCs and the behaviors of compounds that are sensitive to halogen chemistry such as dimethyl sulfide, NO_x, and O_3 in the MBL.

1. Introduction

Reactive halogen chemistry involving sea-salt aerosols is potentially important for determining the behaviors of O_3, NO_x, SO_2, dimethyl sulfide (DMS), and mercury in the marine boundary layer (MBL). Several exploratory modeling studies have indicated that reactive bromine and chlorine species can build up via autocatalytic halogen release from sea-salt aerosols to strongly influence the fate of the above-mentioned species via reactions occurring in the gas phase as well as in aerosols and cloud droplets (Sander and Crutzen, 1996; Vogt et al., 1996; Sander et al., 1999; Toyota et al., 2001; von Glasow et al., 2002a,b; Hedgecock et al., 2003). There also exists circumstantial evidence that reactive halogen chemistry exerts a strong influence on DMS and O_3 loss rates in the air over the ocean, as envisaged from large discrepancies between their mixing ratios modeled without halogen chemistry and those observed (e.g. Chin et al., 1998; Dickerson et al., 1999; Nagao et al., 1999; James et al., 2000; Chand et al., 2003). The autocatalytic halogen release is triggered by scavenging either OH, NO_3, N_2O_5, or O_3 from the gas phase to oxidize Br^- in sea salt (Finlayson-Pitts et al., 1990; Sander and Crutzen, 1996; Hirokawa et al., 1998; Knipping et al., 2000). Caro's acid (HSO_5^-), formed via aqueous-phase radical reactions of S(IV), and inorganic iodine species such as HOI, derived from organic iodines of biogenic origin, are also suggested to be effective in oxidizing sea-salt Br^- (Mozurkewich, 1995; Vogt et al., 1996, 1999). Even though small initially, the amount of reactive bromine thus produced will be increased under sunlight as mediated by a series of reactions in the gas phase and in the acidified sea-salt aerosols (Sander and Crutzen, 1996; Vogt et al., 1996; Sander et al., 1999):

$$Br^- + HOBr + H^+ \rightarrow Br_2 + H_2O \tag{1}$$

$$Cl^- + HOBr + H^+ \rightarrow BrCl + H_2O \tag{2}$$

$$BrONO_2 + Br^- \rightarrow Br_2 + NO_3^- \tag{3}$$

$$BrONO_2 + Cl^- \rightarrow BrCl + NO_3^- \tag{4}$$

Title Page

Abstract | Introduction

Conclusions | References

Tables | Figures

◀◀ | ▶▶

◀ | ▶

Back | Close

Full Screen / Esc

$$BrCl + Br^- \rightleftharpoons Br_2Cl^- \rightleftharpoons Br_2 + Cl^- \qquad (5)$$

$$Br_2 + h\nu \rightarrow Br + Br \qquad (6)$$

$$BrCl + h\nu \rightarrow Br + Cl \qquad (7)$$

$$Br + O_3 \rightarrow BrO + O_2 \qquad (8)$$

5 $$BrO + HO_2 \rightarrow HOBr + O_2 \qquad (9)$$

$$BrO + NO_2 \xrightarrow{M} BrONO_2. \qquad (10)$$
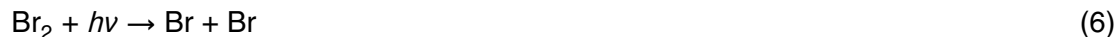
It should be noted that reactive chlorine is also released from sea-salt aerosols in this reaction sequence. Although not definitively, model predictions about the behaviors of inorganic bromine compounds are supported by observational data. During 8 days of

10 a cruise off the west African coast, Rancher and Kritz (1980) collected air samples in the tropical MBL using alkali-impregnated filters. They found that the mixing ratio of inorganic gaseous bromine varied between 1 and 6 pmol/mol at close range to that of particulate bromine for aerosol samples simultaneously obtained. In addition, the mixing ratio of inorganic gaseous bromine was generally higher during the daytime

15 than during the nighttime and that of particulate bromine showed an opposite diurnal trend, implying that a sunlight-induced mechanism is responsible for bromine release from sea-salt aerosols. Using the same technique, Rahn et al. (1976) determined the mixing ratio of inorganic gaseous bromine to be 6.7 pmol/mol for one sample collected at Bermuda. Further support is given by a fact that substantial Br^- loss from sea-salt

20 aerosols is quite common in the mid- and low-latitude remote MBL and closely linked with the availability of acidity in aerosols (Duce et al., 1983; Arimoto et al., 1987, 1990; Ayers et al., 1999; Gabriel et al., 2002). On the other hand, measurements using a Differential Optical Absorption Spectroscopy (DOAS) instrument at Mace Head (the mid-latitude coastal site) determined the mixing ratio of BrO to be always close to or

25 below the detection limit of about 1-2 pmol/mol (James et al., 2000). Leser et al. (2003) deduced the similar range of BrO mixing ratios (generally below the detection limit of <1 to 3.6 pmol/mol with a maximum significant value of 2.4 pmol/mol) in the Atlantic MBL from shipboard DOAS measurements during the cruise from Germany to South

Photochemistry of VOCs and halogens in the MBL

K. Toyota et al.

Title Page

Abstract | Introduction

Conclusions | References

Tables | Figures

◄ | ►

◄ | ►

Back | Close

Full Screen / Esc

Print Version

Interactive Discussion

Africa in October 2000. These rather low levels of BrO mixing ratios are still within the range of model predictions, and besides, capable of doubling the oxidation rates of NO_x and DMS as well as augmenting the photochemical loss rate of O_3 by at least 5-10% in the mid-latitude MBL (Vogt et al., 1996; Ingham et al., 1999; Sander et al., 1999; Toyota et al., 2001).

As mentioned above, the autocatalytic halogen release from sea-salt aerosols is a consequence of interplay between the gas- and aqueous-phase reactions. Therefore the concentrations of gas-phase compounds that are reactive toward halogen species are among the key factors for the buildup of reactive halogens. For instance, model-predicted bromine activation is notably enhanced by varying O_3 mixing ratios from ~10 nmol/mol to ~20 nmol/mol, since Reaction (8) is an important step to give HOBr and $BrONO_2$, key compounds for oxidizing halide ions in the aqueous phase (von Glasow et al., 2002a; Wagner et al., 2002). Reactions between Br atoms and volatile organic compounds (VOCs) will exert an opposite influence on the autocatalytic halogen release by circumventing Reaction (8). To date several studies concerning halogen chemistry in the springtime Arctic boundary layer have addressed the significance of such reactions. For instance, HCHO and CH_3CHO are important for determining the magnitude of "bromine explosion" and its impact on O_3 loss in the springtime Arctic boundary layer, since these aldehydes are fairly abundant there (typically [HCHO] ~200 pmol/mol and [CH_3CHO] ~100 pmol/mol) and highly reactive toward Br atoms to give HBr (Shepson et al., 1996; Sumner and Shepson, 1999). Addition reactions of Br atoms to C_2H_4 and C_2H_2 are also suggested to be effective in impeding the bromine explosion, since they result in the formation of relatively stable brominated intermediates in the organic form; however, the magnitude of their impacts depends strongly on a factor that is not fully characterized, i.e. how stable the reaction products are against subsequent reactions to regenerate inorganic bromine (McConnell et al., 1992; Sander et al., 1997).

Actually, a variety of evidence suggests that oxygenated organic compounds and non-methane hydrocarbons are emitted from the ocean to the overlying atmosphere

(e.g. Ratte et al., 1993; Zhou and Mopper, 1997; Lewis et al., 1999, 2001; Singh et al., 2001). In the remote MBL, the origins of short-lived VOCs such as CH_3CHO and low-molecular-weight alkenes are often dominated by their oceanic emissions with impacts of long-range transport from the continents being marginal (Koppmann et al., 1992; Donahue and Prinn, 1993; Plass-Dülmer et al., 1993; Heikes et al., 1996; Saito et al., 2000; Singh et al., 2001). Previous studies have addressed the impacts of oceanic VOCs emissions within the context of HO_x-NO_x chemistry and/or organic acids formation (e.g. Arlander et al., 1990; Donahue and Prinn, 1990; Singh et al., 2001). However, tropospheric chemical-transport models often neglect or incompletely account for the oceanic emissions of VOCs, thereby underestimating the concentrations of carboxylic acids and carbonyl compounds in the remote marine atmosphere (Baboukas et al., 2000; Singh et al., 2001).

Here we investigate the potential impacts of short-lived VOCs of oceanic origin on reactive halogen chemistry in the MBL by using the multiphase photochemical box model SEAMAC (size-SEgregated Aerosol model for Marine Air Chemistry) (Toyota et al., 2001). The model takes account of a number of reactions for halogen species (Cl_x, Br_x) as well as O_x, HO_x, NO_x, SO_x, CO and hydrocarbon oxidation products in the gas phase and in the deliquesced sea-salt aerosols. For the purpose of this study, the gas-phase reaction scheme is thoroughly updated from that in our previous work to achieve a near-explicit representation of photochemical degradation of up to C_3-hydrocarbons (i.e. CH_4, C_2H_6, C_3H_8, C_2H_4, C_3H_6, and C_2H_2) initiated by reactions with OH radicals, Cl- and Br-atoms, and O_3. In the following sections we will start with reviewing the state of knowledge about the origins of C_2H_4, C_3H_6, and CH_3CHO in the MBL (Sect. 2) and will then describe the new chemical mechanism introduced to SEAMAC (Sect. 3). Then the basic framework of SEAMAC will be briefly described and the details of numerical experiments conducted will be explained (Sect. 4). Finally, results of model runs will be presented and discussed within the context of impacts on halogen activation (Sect. 5).

Title Page

Abstract | Introduction

Conclusions | References

Tables | Figures

◄ | ►

◄ | ►

Back | Close

Full Screen / Esc

Print Version

Interactive Discussion

2. Ethene, propene, and acetaldehyde in the MBL

Seawater concentrations of low-molecular-weight non-methane hydrocarbons and some carbonyl compounds have been found to be supersaturated relative to their concentrations in the overlying air (Lamontagne et al., 1974; Bonsang et al., 1988; Plass et al., 1992; Donahue and Prinn, 1993; Zhou and Mopper, 1997). These compounds are produced primarily via photochemical degradation of dissolved organic carbon of biogenic origin, whereas their direct formation via biological processes is of secondary importance (Ratte et al., 1993, 1998; Zhou and Mopper, 1997). Among the compounds supersaturated in seawater, the origins of relatively long-lived species including C_2H_6, C_3H_8, and C_2H_2 appear to be dominated by long-range transport from the continents even in the remote MBL (Koppmann et al., 1992; Plass-Dülmer et al., 1993). On the other hand, low-molecular-weight alkenes including C_2H_4 and C_3H_6 are almost exclusively derived from their oceanic emissions in the remote MBL (Koppmann et al., 1992; Plass-Dülmer et al., 1993; Heikes et al., 1996). Similarly, Singh et al. (2001) found that the atmospheric mixing ratios of CH_3CHO simulated by a global-scale tropospheric chemical-transport model of Harvard University were lower by about 80-90% than observed over the remote tropical Pacific Ocean, suggesting the presence of missing sources including the oceanic emission.

Table 1 lists the observed mixing ratios of C_2H_4, C_3H_6, and CH_3CHO in the MBL with clean air masses as reported in the recent literature. In the present work, model runs are conducted to cover the ranges of these observed mixing ratios by varying net sea-to-air fluxes of these compounds.

Regarding CH_3CHO, only the work of Zhou and Mopper (1997) has quantitatively assessed its sea-to-air flux by measuring the concentrations in the sea surface microlayer and the underlying bulk seawater of the south Sargasso Sea about 100 km east of the Bahamas. They found that CH_3CHO is significantly enriched in the surface microlayer than in the bulk seawater and that the microlayer enrichment becomes greater during the daytime. Applying these measurements to a diffusive microlayer model, net sea-to-

air flux of CH_3CHO was estimated to be approximately 1.2×10^{10} molecule cm^{-2} s^{-1}. We find that this value is more than enough to give observed CH_3CHO mixing ratios presented in Table 1 under the mid-latitude MBL conditions. Thus oceanic emission rates somewhat smaller than estimated by Zhou and Mopper (1997) are invoked in our model runs (see Sect. 4).

It is interesting to note that a significant enrichment of HCHO in the sea surface microlayer also takes place as a result of its photochemical production during the daytime. Zhou and Mopper (1997) found the molar concentration of HCHO in the sea surface microlayer to be even greater than that of CH_3CHO. However, since the hydration constant of HCHO is three orders of magnitude greater than that of CH_3CHO, HCHO formed in the surface microlayer will be diffused downward to the bulk seawater rather than emitted to the overlying atmosphere. In other words, the sea surface represents a sink for atmospheric HCHO.

Regarding C_2H_4 and C_3H_6, a fairly large number of studies have been performed in attempts to estimate their fluxes from the ocean (see Fig. 1). Methods applied in such estimates can be categorized into two types. The first type of method is a diffusive microlayer approach based on observed seawater concentrations (e.g. Plass-Dülmer et al., 1993), which would be less susceptible to anthropogenic influences than atmospheric concentrations. However, this approach as applied to date might have underestimated the rates of alkene emissions from the ocean, since seawater samples have been generally taken from the bulk subsurface water rather than from the surface microlayer (Lewis et al., 2001). The second type of method is a budget analysis based on observed atmospheric concentrations with the aid of photochemical models (e.g. Heikes et al., 1996). Flux estimates made by Donahue and Prinn (1990) based on this method are extremely greater than other estimates, since the atmospheric data they used are biased toward higher concentrations ($[C_2H_4]$ ~150 pmol/mol, $[C_3H_6]$ ~100 pmol/mol) than those typical of the remote MBL. As suggested by Donahue and Prinn (1993), atmospheric samplings under relatively strong influence of long-range transport from the continents and/or systematic problems with canister sampling would

Title Page

Abstract	Introduction
Conclusions	References
Tables	Figures

◄ | ►

◄ | ►

Back | Close

Full Screen / Esc

Print Version

Interactive Discussion

be probable reasons for high alkene concentrations obtained in some earlier studies. Among the estimates presented in Fig. 1, those made by Plass-Dülmer et al. (1993), Heikes et al. (1996), Thompson et al. (1993), Bonsang (1993), and Donahue and Prinn (1990) are used in our model runs. Under the mid-latitude MBL conditions the first four estimates will generally give the lower-bound to median mixing ratios of alkenes presented in Table 1, whereas the estimates by Donahue and Prinn (1990) will give C_2H_4 and C_3H_6 mixing ratios both in excess of 100 pmol/mol. Although the latter situation would hardly occur in the remote MBL, resultant influence on halogen activation is noteworthy as will be shown later (see Sect. 5).

3. Chemical mechanism development

A number of studies have been conducted to address tropospheric photochemistry of hydrocarbons initiated via reactions with OH, NO_3, and O_3. Relevant kinetic and photochemical parameters for these reactions have been determined by numerous experimental studies and critically evaluated to give recommended values (e.g. Atkinson et al., 1997, 1999), which provide a primary basis for our chemical mechanism development. By supplementing with a protocol based on the version 3 of Master Chemical Mechanism (MCM) (Jenkin et al., 1997; Saunders et al., 2003), a near-explicit chemical mechanism describing the degradation of up to C_3-hydrocarbons is constructed.

Kinetic and mechanistic information on hydrocarbon degradation initiated by halogen atoms has been less characterized in comparison. Nevertheless, kinetic data for the reactions of Cl- and Br-atoms with various low-molecular-weight hydrocarbons and their mechanistic information are becoming available (e.g. Barnes et al., 1989; Wallington et al., 1989; Bierbach et al., 1996; DeMore et al., 1997; Atkinson et al., 1997, 1999). In view of results from laboratory studies identifying reaction products, their degradation pathways possess qualitative similarities to those for OH-initiated reactions (e.g. Barnes et al., 1989; Yarwood et al., 1992; Bierbach et al., 1997). Main difficulties arise in the scarcity of kinetic and mechanistic information on the reactions of halogen-

Photochemistry of VOCs and halogens in the MBL

K. Toyota et al.

Print Version

Interactive Discussion

containing organic oxygenates. They need to be estimated in the majority of cases; however, by extrapolating available information, a near-explicit description of Cl- and Br-initiated degradation of up to C_3-hydrocarbons is also achieved. The methodology applied in MCM helps create a protocol for such reactions as well.

Unfortunately experimental data for aqueous-phase reactions of halogen-containing organic oxygenates are generally lacking. Hence our efforts to develop an updated chemical mechanism are placed mainly on gas-phase chemistry. The uptake of organic acids onto sea-salt aerosols is basically taken into account, although their further degradation via aqueous-phase chemistry are neglected except those for $HCOOH/HCOO^-$. The aerosol uptake of organic hydroperoxides, aldehydes, and ketones is also neglected with a few exceptions. These assumptions may not constitute major drawbacks, since the aqueous solubility of these gases is expected to be fairly low and the liquid water content of sea-salt aerosols would be too small for such compounds to exert a noticeable influence on overall chemistry.

In this section we describe how we have constructed a new chemical mechanism by highlighting the Br- and/or Cl-initiated degradation pathways of each hydrocarbon considered in the present work. Since Cl-initiated degradation of alkenes possess qualitative similarities to Br-initiated counterparts, the descriptions of the former are eliminated from this section and provided in an electronic supplement (http://www.atmos-chem-phys.org/acpd/3/4549/acpd-3-4549_supp.zip) to this paper instead. Complete listings of gas- and aqueous-phase reactions with their rate constants and of relevant parameters (Henry's law constants, mass accommodation coefficients, and equilibrium constants for ion dissociation) for multiphase reactions are also given in the electronic supplement (http://www.atmos-chem-phys.org/acpd/3/4549/acpd-3-4549_supp.zip).

3.1. Alkane degradation initiated by Cl/Br atoms

Chlorine atoms are highly reactive towards alkanes and generally their rate constants are even greater than those for analogous reactions between OH radicals and alkanes.

The reactions will proceed via hydrogen abstraction from alkyl group to give HCl and alkyl peroxy radicals in the ambient air:

$$Cl + CH_4 \overset{O_2}{\to} HCl + CH_3OO \tag{11}$$

$$Cl + C_2H_6 \overset{O_2}{\to} HCl + C_2H_5OO \tag{12}$$

$$5 \quad Cl + C_3H_8 \overset{O_2}{\to} HCl + 0.43 \times CH_3CH_2CH_2OO + 0.57 \times CH_3CH(OO)CH_3. \tag{13}$$

In the present work rate constants for these reactions are taken from those recommended by Atkinson et al. (1999). The product branching ratios of Reaction (13) are taken from experimentally determined values at 296 K (Tyndall et al., 1997).

Alkyl peroxy radicals thus produced will undergo further degradation following the
10 same pathways as those produced via OH-initiated alkane oxidations. Among the degradation products a series of aldehydes, HCHO, CH_3CHO, and C_2H_5CHO, is most noteworthy in terms of autocatalytic halogen release from sea-salt aerosols, since they react quite rapidly with Br atoms to give relatively stable HBr:

$$Br + HCHO \overset{O_2}{\to} HBr + CO + HO_2 \tag{14}$$

$$15 \quad Br + CH_3CHO \overset{O_2}{\to} HBr + CH_3C(O)OO \tag{15}$$

$$Br + C_2H_5CHO \overset{O_2}{\to} HBr + C_2H_5C(O)OO. \tag{16}$$

It should be noted that rate constants for these reactions become progressively greater as the carbon number of alkyl group increases: $k_{15}/k_{14} = 3.60 \pm 0.29$ and $k_{16}/k_{14} = 6.65 \pm 0.53$ over the temperature range 240-300 K (Ramacher et al., 2000).
20 In view of recent observational data for the mixing ratios of HCHO (ca. 300 pmol/mol) and CH_3CHO (ca. 90 pmol/mol) in the remote Pacific lower troposphere (Singh et al., 2001), CH_3CHO is suggested as important as HCHO for impeding autocatalytic halogen release in the MBL (see Sect. 5.2 for further discussion).

Reactions between Br atoms and low-molecular-weight alkanes proceed so slow at
25 atmospheric temperatures that they are of negligible importance in the atmosphere

(Russell et al., 1988). Thus the reactions of Br atoms with CH_4, C_2H_6, and C_3H_8 are neglected in our reaction scheme.

3.2. C_2H_4 degradation initiated by Br atoms

The reaction Br + C_2H_4 will proceed predominantly via addition channel to give $BrCH_2CH_2OO$ radicals in the ambient air:

$$Br + C_2H_4 \xrightarrow{M,O_2} BrCH_2CH_2OO \tag{17}$$

whereas a hydrogen abstraction channel is too endothermic (ΔH_{298} = 23.2 ± 1 kcal/mol) to possess a noticeable rate at ambient temperature (Bedjanian et al., 1999):

$$Br + C_2H_4 \rightarrow HBr + C_2H_3. \tag{18}$$

In the present work the rate constant for Reaction (17) is taken from Ramacher et al. (2001).

Yarwood et al. (1992) performed an FTIR product study for UV-irradiated Br_2/C_2H_4/air mixtures and identified $BrCH_2CHO$, $BrCH_2CH_2OOH$, and $BrCH_2CH_2OH$ as main degradation products where secondary reactions are minimized. This implies that $BrCH_2CH_2OO$ formed via Reaction (17) will undergo qualitatively similar reactions to those of simple peroxy radicals such as CH_3OO. Thus reactions with either NO, HO_2, or CH_3OO are deemed to be the most likely fate of $BrCH_2CH_2OO$ in the ambient air:

$$BrCH_2CH_2OO + NO \rightarrow BrCH_2CH_2O^* + NO_2 \tag{19}$$

$$BrCH_2CH_2OO + HO_2 \rightarrow BrCH_2CH_2OOH + O_2 \tag{20}$$

$$BrCH_2CH_2OO + CH_3OO \rightarrow 0.44 \times (BrCH_2CH_2O + CH_3O + O_2)$$
$$+ 0.28 \times (BrCH_2CHO + CH_3OH) + 0.28 \times (BrCH_2CH_2OH + HCHO). \tag{21}$$
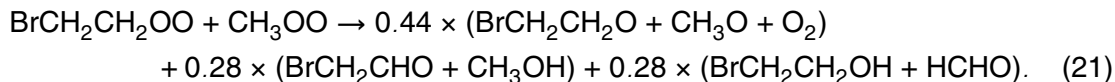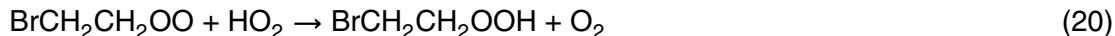
Unfortunately, kinetic and mechanistic data do not exist except the self-reaction of $BrCH_2CH_2OO$ and are therefore estimated as described in Sect. 3.5. Here it should

be noted that kinetic and mechanistic nature of the reactions of $BrCH_2CH_2OO$ with NO, HO_2, and CH_3OO are assumed generally identical to those of $ClCH_2CH_2OO$ (see also Sect. S1 of the electronic supplement, http://www.atmos-chem-phys.org/acpd/3/4549/acpd-3-4549_supp.zip). There are two justifications for this assumption.

5 Firstly, Yarwood et al. (1992) also performed an FTIR product analysis for UV-irradiated Cl_2/C_2H_4/air mixtures and found that main degradation products are $ClCH_2CHO$, $ClCH_2CH_2OOH$, and $ClCH_2CH_2OH$ with the yields identical to those of $BrCH_2CHO$, $BrCH_2CH_2OOH$, and $BrCH_2CH_2OH$ formed from UV-irradiated Br_2/C_2H_4/air mixtures. Secondly, rate constants for the self-reactions of $BrCH_2CH_2OO$ ($k = 4.0 \times$

10 $10^{-12}\,cm^3\,molecule^{-1}\,s^{-1}$) and of $ClCH_2CH_2OO$ ($k = 3.3 \times 10^{-12}\,cm^3\,molecule^{-1}\,s^{-1}$) are fairly close to each other, being more than an order of magnitude greater than that for the self-reaction of C_2H_5OO (Crowley and Moortgat, 1992; Villenave et al., 2003). The slight difference between the rate constants for the self-reactions of $BrCH_2CH_2OO$ and of $ClCH_2CH_2OO$ results in a somewhat greater rate constant estimated for Re-

15 action (21) than that for the analogous cross-reaction $ClCH_2CH_2OO + CH_3OO$ (see Sect. 3.5).

By analogy with the fate of $HOCH_2CH_2O$ radicals produced via OH-initiated C_2H_4 oxidation, alkoxy radicals ($BrCH_2CH_2O^*$ and $BrCH_2CH_2O$) formed via Reactions (19) and (21) can either decompose to give $BrCH_2 + HCHO$ or react with O_2 to give $BrCH_2CHO$

20 $+ HO_2$. However, in view of fairly good mass balance between C_2H_4 reacted and the three main products containing bromine in the experiments performed by Yarwood et al. (1992), it is quite likely that $BrCH_2CH_2O$ radicals formed via Reaction (21) exclusively react with O_2:

$$BrCH_2CH_2O + O_2 \rightarrow BrCH_2CHO + HO_2. \tag{22}$$

25 On the other hand, recent experimental studies identified several examples for chlorinated and/or brominated alkoxy radicals produced via reactions between their parent peroxy radicals and NO to decompose before thermalized, since alkoxy radicals thus produced will possess internal excitation due to the exothermicity of reactions (Bilde

et al., 1998, 1999; Orlando et al., 1998). However, it is completely unknown whether Reaction (19) gives internally excited $BrCH_2CH_2O^*$, since previous product studies for Br-initiated C_2H_4 degradation have not been conducted with added NO to facilitate Reaction (19) (Barnes et al., 1989; Yarwood et al., 1992). The fate of $BrCH_2CH_2O^*$, if

5 formed, is also unknown. In the present work it is tentatively assumed that Reaction (19) does give $BrCH_2CH_2O^*$ and that the further degradation of $BrCH_2CH_2O^*$ occurs analogously to that of $ClCH_2CH_2O^*$ (see Sect. S1):

$$BrCH_2CH_2O^* \xrightarrow{O_2} 0.58 \times (BrCH_2CHO + HO_2) + 0.42 \times (BrCH_2OO + HCHO). \qquad (23)$$
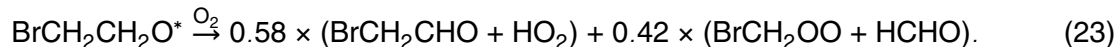
The reactions of $BrCH_2OO$ have been characterized relatively well. Rate constants

10 and product branching ratios for its reactions with NO, HO_2, and itself have been measured or derived experimentally (Sehested et al., 1993; Chen et al., 1995; Villenave and Lesclaux, 1995). Such information well delineates the fate of $BrCH_2OO$ in the ambient air:

$$BrCH_2OO + NO \rightarrow BrCH_2O^* + NO_2 \qquad (24)$$

15 $$BrCH_2OO + HO_2 \rightarrow 0.9 \times (BrCH_2OOH + O_2) + 0.1 \times (HCOBr + H_2O + O_2) \qquad (25)$$

$$BrCH_2OO + CH_3OO$$
$$\rightarrow 0.65 \times (BrCH_2O + CH_3O + O_2) + 0.35 \times (BrCH_2OH + HCHO) \qquad (26)$$
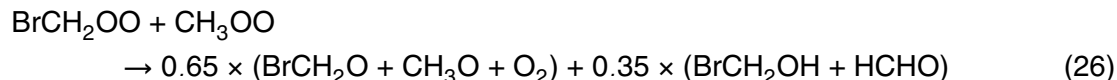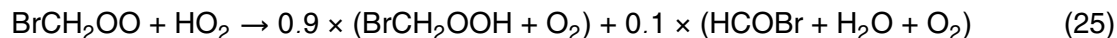
where the rate constant and the branching ratios for Reaction (26) are estimated as described in Sect. 3.5.

20 The fate of $BrCH_2O$ (or $BrCH_2O^*$) radicals has been addressed by experimental studies in the context of atmospheric chemistry of CH_3Br initiated by OH- or Cl-attack (Nielsen et al., 1991; Weller et al., 1992; Chen et al., 1995; Orlando et al., 1996). The formation of HCOBr is generally observed in the absence of NO in the reaction systems, which was attributed to a reaction between $BrCH_2O$ and O_2 by Nielsen et al.

25 (1991) and Weller et al. (1992):

$$BrCH_2O + O_2 \rightarrow HCOBr + HO_2. \qquad (27)$$

The yields of HCOBr were suppressed to levels lower than detection limits by adding NO to the reaction systems (Weller et al., 1992; Chen et al., 1995; Orlando et al., 1996), which can be deemed to represent a piece of evidence for internally excited $BrCH_2O^*$ radicals formed via Reaction (24) decomposing before reacting with O_2:
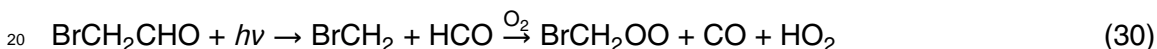
$$BrCH_2O^* \rightarrow HCHO + Br. \tag{28}$$

However, Chen et al. (1995) and Orlando et al. (1996) found the independence of the HCOBr yield on O_2 partial pressure even in the absence of NO, and thus concluded that HCOBr observed in the absence of NO was likely to be formed via Reaction (25) rather than via Reaction (27). In the present work $BrCH_2O$ is assumed to undergo either Reaction (27) or decomposition via Br-atom elimination:

$$BrCH_2O \rightarrow HCHO + Br \tag{29}$$

where $k_{27} = 6 \times 10^{-14}$ cm^3 molecule^{-1} s^{-1} and $k_{29} = 3 \times 10^7$ s^{-1}, respectively (Orlando et al., 1996). It follows that approximately 99% of $BrCH_2O$ loss occurs via Reaction (29) in 1 atm of air. On the other hand, $BrCH_2O^*$ radicals are assumed to exclusively undergo decomposition via Reaction (28).

Kinetic and mechanistic data for the degradation reactions of brominated organic intermediates are severely limited. Therefore the fate of this class of compounds is described mostly on the basis of estimated reaction rates as mentioned below.

In the ambient air $BrCH_2CHO$ will be destroyed via either photolysis or OH attack:

$$BrCH_2CHO + h\nu \rightarrow BrCH_2 + HCO \xrightarrow{O_2} BrCH_2OO + CO + HO_2 \tag{30}$$
$$\rightarrow CH_3Br + CO \tag{31}$$
$$BrCH_2CHO + OH \rightarrow BrCH_2CO + H_2O. \tag{32}$$
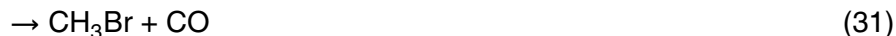
The rate constant for Reaction (32) as well as absorption cross sections and quantum yields for $BrCH_2CHO$ photolysis are unknown at the present time; they are estimated as described in section 3.6. The formation of $CH_3Br + CO$, i.e. Reaction (31), is assumed

to occur as a minor channel of $BrCH_2CHO$ photolysis. $BrCH_2CO$ radicals formed via Reaction (32) will be lost via three different pathways:

$$BrCH_2CO + O_2 \xrightarrow{M} BrCH_2C(O)OO \tag{33}$$

$$BrCH_2CO \xrightarrow{M} BrCH_2 + CO \xrightarrow{O_2} BrCH_2OO + CO \tag{34}$$

$$\xrightarrow{M} Br + CH_2=CO \tag{35}$$
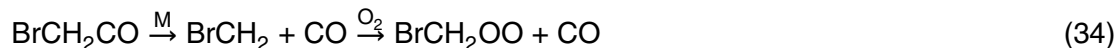
where the branching ratios of Reactions (33), (34), and (35) are 0.5, 0.25, and 0.25, respectively, at 297 K in 700 Torr of air (Chen et al., 1996). $BrCH_2C(O)OO$ radicals thus produced will undergo reactions analogous to those of $CH_3C(O)OO$, giving various products including $BrCH_2(O)OONO_2$ (PBrAN), $BrCH_2COOH$, and $BrCH_2C(O)OOH$:

$$BrCH_2C(O)OO + NO_2 \underset{}{\overset{M}{\rightleftharpoons}} BrCH_2(O)OONO_2 \tag{36}$$

$$BrCH_2C(O)OO + NO \xrightarrow{M,O_2} BrCH_2OO + CO_2 + NO_2 \tag{37}$$

$$BrCH_2C(O)OO + HO_2 \rightarrow$$
$$0.71 \times (BrCH_2C(O)OOH + O_2) + 0.29 \times (BrCH_2COOH + O_3) \tag{38}$$

$$BrCH_2C(O)OO + CH_3OO \xrightarrow{M,O_2} 0.7 \times (BrCH_2OO + CO_2 + HCHO + HO_2 + O_2)$$
$$+ 0.3 \times (BrCH_2COOH + HCHO + O_2). \tag{39}$$
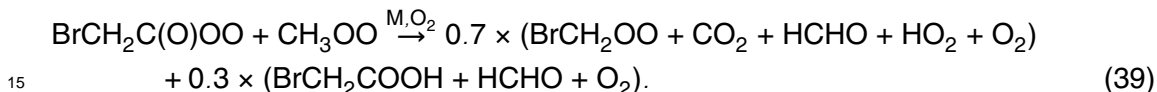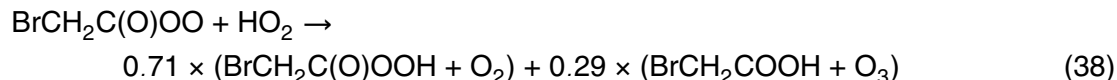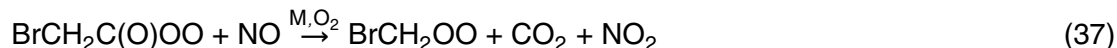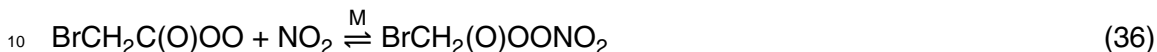
The formation of these compounds has been verified experimentally: PBrAN formed from Br-atom initiated oxidation of $BrCH_2CHO$ in the NO_2-rich air (Chen et al., 1996); $BrCH_2COOH$ and possibly $BrCH_2C(O)OOH$ formed from Br-atom initiated oxidation of C_2H_4 in the air without added NO_2 (Barnes et al., 1989). However, the rate constants and product yields of Reactions (36)–(39) are unknown and therefore assumed identical to those of analogous reactions for $CH_3C(O)OO$ radicals.

In the actinic range absorption cross sections for HCOBr are more than an order of magnitude greater than those for HCOCl (Libuda, 1992). Given that a quantum yield for HCOBr photolysis is unity, the lifetime of HCOBr against photolysis is estimated to

be about 6.5 days in the mid-latitude MBL (see Table S2 of the electronic supplement, http://www.atmos-chem-phys.org/acpd/3/4549/acpd-3-4549_supp.zip):

$$HCOBr + h\nu \xrightarrow{O_2} Br + CO + HO_2. \tag{40}$$
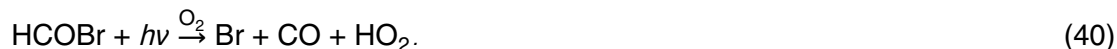
Although the rate constants of OH- and Cl-attacks against HCOBr are unknown at the present time, they are quite likely similar to those of OH- and Cl-attacks against HCOCl (resultant lifetime will be longer than 45 days; see Sect. S1) and therefore of minor importance compared with HCOBr photolysis. On the other hand, previous experimental studies reported that HCOBr is highly susceptible to a wall reaction on the chamber surface to give HBr + CO (Weller et al., 1992; Chen et al., 1995; Orlando et al., 1996). An analogous wall reaction of HCOCl also takes place on the chamber surface (Libuda et al., 1990; Kaiser and Wallington, 1994; Wallington et al., 1996). On the basis of experimental evidence that non-hydrolytic decay of HCOCl to give HCl + CO occurs quite rapidly in aqueous solutions (Dowideit et al., 1996), the reactive uptake coefficient of HCOCl on the surface of sea-salt aerosols is estimated to be 0.1 in the present work (see further discussion in Sect. S1). The same uptake coefficient is assumed to apply to HCOBr, constraining its lifetime in the MBL to be on the order of hours.

Brominated hydroperoxides will be destroyed via either OH attacks or photolysis, although no experimental data exist for these reactions. As for $BrCH_2CH_2OOH$, the following pathways are considered:

$$OH + BrCH_2CH_2OOH \rightarrow H_2O + BrCH_2CH_2OO \tag{41}$$
$$\rightarrow H_2O + BrCH_2CHO + OH \tag{42}$$
$$BrCH_2CH_2OOH + h\nu \rightarrow BrCH_2CH_2O + OH. \tag{43}$$
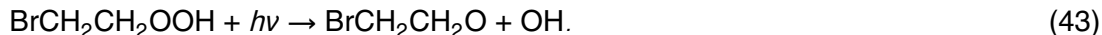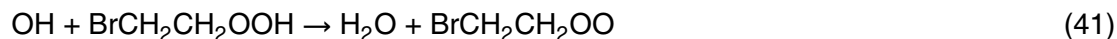
Similarly, $BrCH_2OOH$ will be destroyed via the following pathways:

$$OH + BrCH_2OOH \rightarrow H_2O + BrCH_2OO \tag{44}$$
$$\rightarrow H_2O + HCOBr + OH \tag{45}$$
$$BrCH_2OOH + h\nu \rightarrow BrCH_2O + OH. \tag{46}$$

Title Page

Abstract | Introduction

Conclusions | References

Tables | Figures

◀◀ | ▶▶

◀ | ▶

Back | Close

Full Screen / Esc

Print Version

Interactive Discussion

Rate constants or J values for Reactions (41)–(46) are estimated as described in Sect. 3.6. Actually, the OH attack on $BrCH_2CH_2OOH$ may have an additional channel to give $BrCHCH_2OOH + H_2O$. It is estimated, however, of minor importance compared with channels (41) and (42), and therefore neglected in the present work. Then the rate constant of Reaction (42) is scaled to maintain the overall rate of the OH attack (see Sect. 3.6).
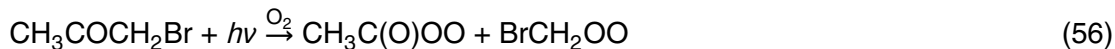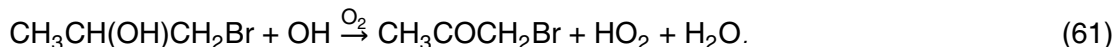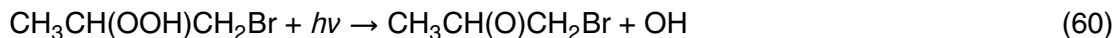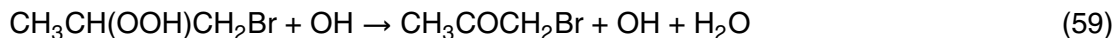
Finally, brominated alcohols will be destroyed via reactions with OH radicals:

$$OH + BrCH_2CH_2OH \xrightarrow{O_2} H_2O + BrCH_2CHO + HO_2 \qquad (47)$$

$$OH + BrCH_2OH \xrightarrow{O_2} H_2O + HCOBr + HO_2 \qquad (48)$$
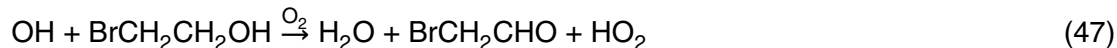
where rate constants are estimated as described in Sect. 3.6 and channels of minor importance are neglected as in the case of brominated hydroperoxides. $BrCH_2OH$ is also quite likely to undergo rapid unimolecular decomposition to give $HCHO + HBr$ by analogy with $ClCH_2OH$ (Tyndall et al., 1993).

3.3. C_3H_6 degradation initiated by Br atoms

The reaction $Br + C_3H_6$ will proceed predominantly via Br-atom addition to the double bond:

$$Br + C_3H_6 \xrightarrow{M,O_2} 0.87 \times CH_3CH(OO)CH_2Br + 0.13 \times CH_3CHBrCH_2OO \qquad (49)$$
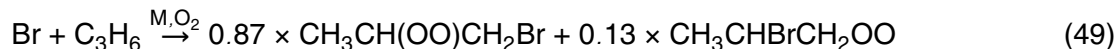
where product branching ratios are assigned by analogy with Cl-atom addition to C_3H_6 (see Sect. S2 in the electronic supplement, http://www.atmos-chem-phys.org/acpd/3/ 4549/acpd-3-4549_supp.zip). In the present work the second-order rate coefficients in 1 atm of air at room temperature obtained by two independent experimental studies (Barnes et al., 1989; Wallington et al., 1989) are averaged and then used for Reaction (49). It is important to note that the rate constant of this reaction is approximately 20 times greater than that of Reaction (17) in 1 atm of air. The rate constant of H-

abstraction from the methyl group by Br atoms has also been determined experimentally (Bedjanian et al., 1998):

$$Br + C_3H_6 \xrightarrow{O_2} HBr + CH_2{=}CHCH_2OO, \tag{50}$$

although the probability of this channel in the overall reaction $Br + C_3H_6$ is less than 1% in 1 atm of air.

CH$_3$CH(OO)CH$_2$Br radicals formed via Reaction (49) will be lost via reactions with NO, HO$_2$, or CH$_3$OO in the ambient air. However, their rate constants are currently unknown and therefore estimated as described in Sect. 3.5:

$$CH_3CH(OO)CH_2Br + NO \rightarrow CH_3CH(O)CH_2Br^* + NO_2 \tag{51}$$

$$CH_3CH(OO)CH_2Br + HO_2 \rightarrow CH_3CH(OOH)CH_2Br + O_2 \tag{52}$$

$$CH_3CH(OO)CH_2Br + CH_3OO \rightarrow 0.6 \times (CH_3CH(O)CH_2Br + CH_3O)$$
$$+ 0.2 \times (CH_3COCH_2Br + CH_3OH) + 0.2 \times (CH_3CH(OH)CH_2Br + HCHO) \tag{53}$$
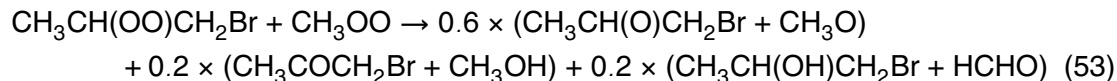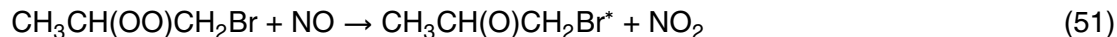
where the product branching ratios of Reaction (53) are taken from generic values assigned in the work of MCM. To date no experimental study has been performed in an attempt to resolve complete pathways of Br-initiated C_3H_6 degradation. Impey et al. (1997), however, determined the yield of bromoacetone (CH$_3$COCH$_2$Br) from the reaction $Br + C_3H_6$ in NO-rich air to be 0.75. From their data and our assumed product branching ratios for Reaction (49), it is estimated that CH$_3$CH(O)CH$_2$Br* radicals undergo decomposition and reaction with O$_2$ with the branching ratios of 0.14 and 0.86, respectively:

$$CH_3CH(O)CH_2Br^* \rightarrow CH_3CHO + BrCH_2 \xrightarrow{O_2} CH_3CHO + BrCH_2OO \tag{54}$$

$$CH_3CH(O)CH_2Br^* + O_2 \rightarrow CH_3COCH_2Br + HO_2. \tag{55}$$
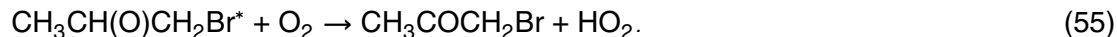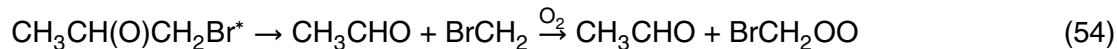
CH$_3$CH(O)CH$_2$Br radicals formed via Reaction (53) are assumed to undergo the same fate as above, since no experimental data exist ruling out this assumption. Actually,

analogous reactions of 3-bromo-2-butoxy ($CH_3CH(O)CHBrCH_3$) radicals were investigated by Bierbach et al. (1997) in their FTIR product study of Br-initiated oxidation of *trans*-2-C_4H_8 in the 1000 mbar air. At 298 K approximately 40% of $CH_3CH(O)CHBrCH_3$ radicals were found to undergo decomposition to give $CH_3CHO + CH_3CHBr$ rather than

5 reaction with O_2 to give $CH_3COCHBrCH_3 + HO_2$, whether NO is added or not to the reaction system.

CH_3COCH_2Br will be destroyed via either photolysis or OH attack in the ambient air. Based on experimentally determined data for the absorption cross sections of CH_3COCH_2Br and quantum yields for its photolysis (Burkholder et al., 2002), the life-

10 time of CH_3COCH_2Br against photolysis is estimated to be less than half a day in the mid-latitude MBL (see Table S2):

$$CH_3COCH_2Br + h\nu \overset{O_2}{\rightarrow} CH_3C(O)OO + BrCH_2OO \qquad (56)$$

$$\overset{O_2}{\rightarrow} CH_3OO + BrCH_2CO. \qquad (57)$$

$BrCH_2OO$ and $BrCH_2CO$ radicals are also formed from Br-initiated C_2H_4 degradation

15 and their fate is already described in Sect. 3.2. The OH attack on CH_3COCH_2Br, whose rate constant is estimated as described in Sect. 3.6, will take place much slower than photolysis.

Experimental data for OH attacks on and/or photolysis of $CH_3CH(OOH)CH_2Br$ and $CH_3CH(OH)CH_2Br$ are lacking at the present time and therefore estimated as de-

20 scribed in Sect. 3.6. Photochemical loss of these species gives either CH_3COCH_2Br or its precursors ($CH_3CH(OO)CH_2Br$ and $CH_3CH(O)CH_2Br$):
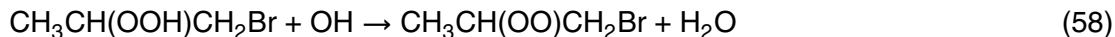
$$CH_3CH(OOH)CH_2Br + OH \rightarrow CH_3CH(OO)CH_2Br + H_2O \qquad (58)$$

$$CH_3CH(OOH)CH_2Br + OH \rightarrow CH_3COCH_2Br + OH + H_2O \qquad (59)$$

$$CH_3CH(OOH)CH_2Br + h\nu \rightarrow CH_3CH(O)CH_2Br + OH \qquad (60)$$

25 $$CH_3CH(OH)CH_2Br + OH \overset{O_2}{\rightarrow} CH_3COCH_2Br + HO_2 + H_2O. \qquad (61)$$

There exist no experimental data concerning Br-initiated C_3H_6 degradation that follows $CH_3CHBrCH_2OO$ formation via Reaction (49). Therefore, kinetics and mechanisms of reactions for this pathway are virtually completely estimated by methods described in Sects. 3.5–3.6.

3.4. C_2H_2 degradation initiated by Cl/Br atoms

Rate constants for reactions Cl/Br + C_2H_2 have been measured by several workers. In the present work, parameters to yield the pseudo-second-order rate constant for the reaction Cl + C_2H_2 are taken from recommended values given by Atkinson et al. (1999), whereas the second-order rate constant for the reaction Br + C_2H_2 measured over 239–296 K in 700 Torr air (Ramacher et al., 2001) is fitted in the Arrhenius form. In the ambient air these reactions are likely to proceed in a similar way to reaction OH + C_2H_2: the formation of X-C_2H_2 adducts (X = Cl, Br) followed by O_2-addition to give XCH=CHOO radicals, which further undergo isomerization and decomposition to form either HCO + HCOX, HCOCHO + X, or HX + HCO + CO (Barnes et al., 1989; Yarwood et al., 1991; Ramacher et al., 2001):

$$X + C_2H_2 \overset{M,O_2}{\rightarrow} XCH=CHOO \tag{62}$$

$$XCH=CHOO \rightarrow HCOX + HCO \overset{O_2}{\rightarrow} HCOX + CO + HO_2 \tag{63}$$

$$\rightarrow HCOCHO + X \tag{64}$$

$$\rightarrow HX + HCO + CO \overset{O_2}{\rightarrow} HX + 2\,CO + HO_2. \tag{65}$$
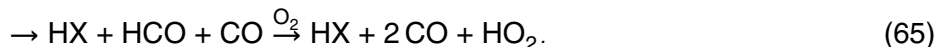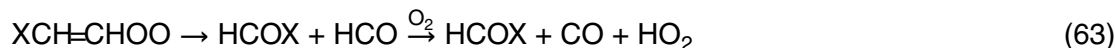
The branching ratios of these pathways are not sensitive to the NO concentration but slightly to temperature (Ramacher et al., 2001). Actually, two geometric isomers exist for XCH=CHOO radicals, i.e. *cis*-XCH=CHOO and *trans*-XCH=CHOO, and the reaction of the former with O_2 to give O_3 (Reaction (66)) may well compete with isomerization/decomposition (63)–(65) in the ambient air (Yarwood et al., 1991; Zhu et al., 1994):
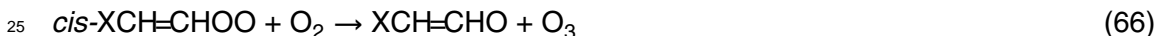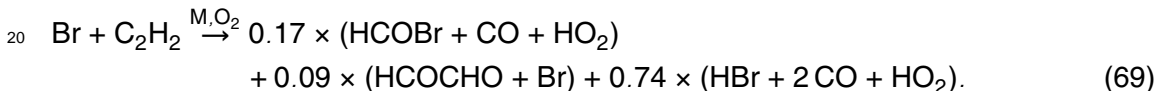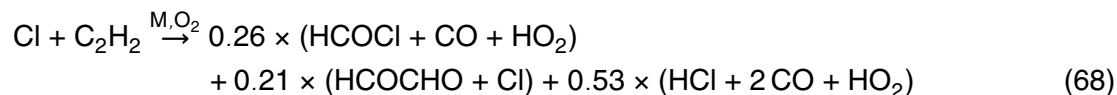
$$\textit{cis}\text{-XCH=CHOO} + O_2 \rightarrow XCH=CHO + O_3 \tag{66}$$

where the yield of O_3 from C_2H_2 reacted is dependent on O_2 partial pressure and is on the order of 0.1 at 296 K in 700 Torr air for both of Cl- and Br-initiated reactions. XCH=CHO radicals, formed along with O_3, will then react with O_2 to give HCOX + CO + OH:

$$XCH=CHO + O_2 \overset{isom./dec.}{\cdots\rightarrow} HCOX + CO + OH. \tag{67}$$
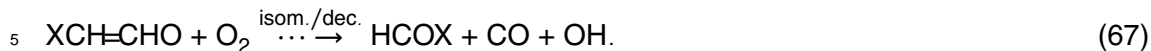
It appears, however, that the formation of O_3 via reaction (66) is of negligible importance for O_3 budget in the MBL; taking the upper limits for reactant concentrations as $[C_2H_2] = 100$ pmol/mol (Gregory et al., 1996), $[Cl] = 10^5$ molecule/cm^3 (Graedel and Keene, 1995), and $[Br] = 10^7$ molecule/cm^3 (Dickerson et al., 1999), and assuming the yields of O_3 from both of the reactions Cl/Br + C_2H_2 to be 0.1, the rate of O_3 production is estimated to be not more than 5 pmol/mol/day at 298 K in 1 atm of air. Considering further the rapid exchange between OH- and HO_2-radicals occurring in the ambient air, the reaction products of O_3-forming pathway via Reactions (66)–(67) are virtually equivalent to those of Reaction (63).

In the present work the branching ratios of reactions Br/Cl + C_2H_2 are taken from the values as derived in the FTIR product study performed by Yarwood et al. (1991) at 296 K in 700 Torr air by disregarding the contributions from O_3-forming pathways:

$$Cl + C_2H_2 \overset{M,O_2}{\rightarrow} 0.26 \times (HCOCl + CO + HO_2)$$
$$+ 0.21 \times (HCOCHO + Cl) + 0.53 \times (HCl + 2\,CO + HO_2) \tag{68}$$

$$Br + C_2H_2 \overset{M,O_2}{\rightarrow} 0.17 \times (HCOBr + CO + HO_2)$$
$$+ 0.09 \times (HCOCHO + Br) + 0.74 \times (HBr + 2\,CO + HO_2). \tag{69}$$

3.5. Kinetics and mechanisms for the reactions of halogen-containing organic peroxy radicals

As described in the preceding sections, the most likely fate of halogen-containing organic peroxy radicals in the ambient air is reactions with either NO, HO_2, or CH_3OO

Photochemistry of VOCs and halogens in the MBL

K. Toyota et al.

radicals. However, relevant kinetic and mechanistic data are lacking in the majority of cases. A protocol for estimating the rate constants for reactions of chlorinated organic peroxy radicals with NO and HO_2 is available in the work of MCM (Saunders et al., 2003). Thus, where no experimental data exist, their rate constants are estimated fol-
lowing the MCM protocol. Here the same protocol is assumed to apply to the reactions of brominated organic peroxy radicals with NO and HO_2.

Kinetic and mechanistic data for the reactions of halogenated organic peroxy radicals with CH_3OO are lacking except for a reaction $ClCH_2OO + CH_3OO$ (Villenave and Lesclaux, 1996). Madronich and Calvert (1990) proposed an empirical approach to
estimate rate constants and product branching ratios for cross-reactions between organic peroxy radicals (so-called permutation reactions) where their experimental data exist for each of self-reactions. This approach has been proved to work fairly well at least for the reaction $ClCH_2OO + CH_3OO$ (Villenave and Lesclaux, 1996), and is therefore adopted for estimating kinetics and mechanisms for this class of reactions in the
present work. Here kinetic and mechanistic data for self-reactions of $ClCH_2CH_2OO$, $BrCH_2CH_2OO$, and $BrCH_2OO$ are taken from experimentally determined values (Lightfoot et al., 1992; Yarwood et al., 1992; Villenave and Lesclaux, 1995; Villenave et al., 2003). Rate constants for self-reactions of $CH_3CH(OO)CH_2Cl$ and $CH_3CH(OO)CH_2Br$ are estimated following a protocol proposed by Villenave et al. (2003). As to the other
halogenated organic peroxy radicals, no experimental basis currently exists to predict kinetics and mechanisms even for their self-reactions. For such species, rate constants and product branching ratios of cross-reactions with CH_3OO are taken from generic values assigned in the work of MCM (Saunders et al., 2003).

3.6. Degradation of organic intermediates: hydroperoxides, aldehydes, ketones, alcohols, etc.

By analogy with non-halogenated compounds, halogenated organic hydroperoxides, percarboxylic acids, aldehydes, ketones, and alcohols are most likely destroyed via either reactions with OH radicals or photolysis in the ambient air. However, kinetic and

mechanistic data for such reactions are again lacking in many cases and thus need to be estimated.

Where no experimental data exist, rate constants for the reactions of halogenated organic intermediates with OH radicals are estimated by structure-activity relation-ships (SAR) (Atkinson, 1987; Kwok and Atkinson, 1995) with supplemented param-eters taken from the work of MCM. In particular, the neighboring group activation pa-rameter for '-OOH' for the purpose of reaction rate estimation is assigned to be 13 for C_1-species and 8.4 for C_2- and C_3-species following the MCM protocol (Jenkin et al., 1997; Saunders et al., 2003). The rate constant of hydrogen abstraction from '-OOH' group is also taken from Jenkin et al. (1997). Actually, there often exist more than two distinct product channels for hydrogen abstraction from the C–H bonds of C_2- and C_3-species. Although the SAR method is capable of predicting the rate constant of each channel, channels of minor importance are disregarded and the rate constant of primary channel is scaled proportionally to maintain the overall rate. This should be a reasonable compromise to avoid making the reaction scheme too much complicated, considering the dearth of experimental data.

Photochemical loss of halogenated and non-halogenated organic intermediates via reactions with Cl, Br, or NO_3 is taken into account only where experimental data exist. Since these reactions are generally of minor importance for the budget of organic inter-mediates considered, mechanism extrapolation is not basically performed for reactions for which no experimental data exist.

Photolysis reactions are considered for halogenated carbonyls (RC(O)R' and RCHO), hydroperoxides (ROOH), and percarboxylic acids (RC(O)OOH), as with non-halogenated counterparts. Again, experimental data for their absorption cross sections in the actinic range are lacking in many cases. Thus, where no experimental data exist, J values for halogenated organic compounds need to be estimated.

As shown in Figs. 2a-b, the longer-wavelength tails of UV absorption bands for car-bonyl compounds are shifted in a fairly consistent manner by the presence of sub-stituents at α-position: blue-shifted by about 10 nm via OH-substitution and red-shifted

by about 10–30 nm via Cl- or Br-substitution. Absorption cross sections for $ClCH_2CHO$ were determined experimentally (Libuda, 1992), whereas those for $BrCH_2CHO$ are unknown at the present time. The quantum yields of $ClCH_2CHO/BrCH_2CHO$ photolysis are also unknown. In the present work, absorption cross sections for $BrCH_2CHO$ are estimated to be red-shifted by 10 nm relative to those for $ClCH_2CHO$. Then, wavelength-dependent quantum yields for two channels of CH_3CHO photolysis to give $CH_4 + CO$ and $CH_3 + HCO$, respectively, recommended by Atkinson et al. (1997) are used as a reference for estimating quantum yields of haloacetaldehyde photolysis; wavelength-dependent quantum yields of the photolysis of $ClCH_2CHO$ and $BrCH_2CHO$ are estimated to be red-shifted by 10 nm and 20 nm, respectively, relative to those of CH_3CHO photolysis. Similarly, J values for other halogen-substituted alkyl aldehydes are estimated by taking absorption cross sections of non-halogenated counterparts from the literature and then red-shifted by 10 nm for chlorinated aldehydes and by 20 nm for brominated aldehydes. Wavelength-dependent quantum yields are red-shifted accordingly. J values for halogenated ketones of interest in the present work, i.e. CH_3COCH_2Cl and CH_3COCH_2Br, are calculated based on experimentally determined absorption cross sections and quantum yields (Burkholder et al., 2002).

To our knowledge, experimental data for absorption cross sections in the actinic range do not exist for hydroperoxides other than CH_3OOH and $HOCH_2OOH$ (Atkinson et al., 1999; Bauerle and Moortgat, 1999). A comparison between their absorption cross sections reveals that the longer-wavelength tails of UV absorption bands for hydroperoxides exhibit no discernible change by the presence of substituents (see Fig. 2c). It is therefore assumed that absorption cross sections for halogenated hydroperoxides are identical to those for CH_3OOH. Then the quantum yields of unity are assumed as with CH_3OOH photolysis. Following the MCM protocol for estimating J values for non-halogenated compounds (Jenkin et al., 1997), halogenated percarboxylic acids (RC(O)OOH) are also assumed to have the same J value as CH_3OOH.
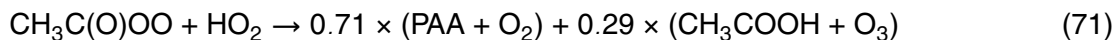
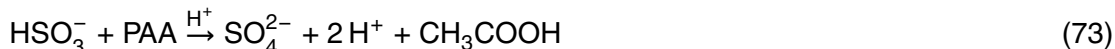## 3.7. Aqueous-phase reactions of peroxyacetic acid (PAA)

Reactions of OH/NO$_3$/Br/Cl with CH$_3$CHO will proceed predominantly via abstraction of aldehydic-H to give CH$_3$C(O)OO radicals in the ambient air (Atkinson et al., 1999):

$$X + CH_3CHO \xrightarrow{O_2} HX + CH_3C(O)OO \qquad (70)$$

5 where X is either OH, NO$_3$, Br, or Cl. In the remote MBL where NO$_x$ concentrations are relatively low, a fairly large fraction of CH$_3$C(O)OO radicals will react with HO$_2$/CH$_3$OO radicals rather than with NO$_x$ to give CH$_3$C(O)OOH (peroxyacetic acid, or PAA) and/or CH$_3$COOH (Jenkin et al., 1997; Atkinson et al., 1999; Saunders et al., 2003):

$$CH_3C(O)OO + HO_2 \rightarrow 0.71 \times (PAA + O_2) + 0.29 \times (CH_3COOH + O_3) \qquad (71)$$

10 $$CH_3C(O)OO + CH_3OO \xrightarrow{O_2}$$
$$0.7 \times (CH_3OO + CO_2 + HCHO + HO_2) + 0.3 \times (CH_3COOH + HCHO + O_2). \quad (72)$$
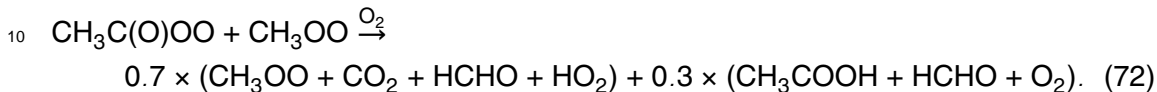
Henry's law constants and acid dissociation constants in water have been determined experimentally for both CH$_3$COOH and PAA so that their uptake onto sea-salt aerosols can be simulated quite reasonably. In addition, rate coefficients for the aqueous-phase
15 oxidation of S(IV), Br$^-$, and Cl$^-$ by PAA have been experimentally determined (Fortnum et al., 1960; Lind et al., 1987), allowing quantitative estimates of their impacts:

$$HSO_3^- + PAA \xrightarrow{H^+} SO_4^{2-} + 2H^+ + CH_3COOH \qquad (73)$$
$$Br^- + PAA \rightarrow BrO^- + CH_3COOH \qquad (74)$$
$$Cl^- + PAA \rightarrow ClO^- + CH_3COOH. \qquad (75)$$

20 Pandis and Seinfeld (1989), using a numerical model, demonstrated that Reaction (73) does not play a major role in cloudwater chemistry. However, the latter two Reactions (74)–(75) are potentially important for triggering autocatalytic halogen release. In our base model run in which the gas-phase mixing ratio of PAA is simulated to be approximately 80 pmol/mol, the contributions from Reactions (74)–(75) are in the same range

as that from $Br^- + O_3$ and about a few percent of those from $Br^-/Cl^- + HSO_5^-$ (see Sect.5.6).

4. Model description and experimental settings

Numerical experiments in the present work are performed by the box model SEAMAC,
5 which describes chemistry of O_x, HO_x, NO_y, SO_x, Cl_x, Br_x species, hydrocarbons, and their oxidation products in the gas phase and in the deliquesced sea-salt aerosols occurring in the MBL of 1 km thickness (Toyota et al., 2001). SEAMAC owes its basic architecture to the ASAD atmospheric chemistry integration package (Carver et al., 1997), which allows flexible modifications of reaction scheme. As described in the
10 previous section, the reaction scheme is updated to achieve a near-explicit description of degradation of up to C_3-hydrocarbons. Consequently, the model includes 199 gas-phase species undergoing 645 reactions and 100 aqueous-phase species undergoing 279 reactions. Chemical interactions between the gas- and aerosol-phases are treated as reversible mass transfer (43 species), irreversible uptake onto aerosols (1
15 species: H_2SO_4), or heterogeneous surface reactions on aerosols (10 species). Kinetic parameters have also been updated from those in our previous work (Toyota et al., 2001), where new experimental data are available (see the electronic supplement (http://www.atmos-chem-phys.org/acpd/3/4549/acpd-3-4549_supp.zip) for a full account of reactions considered in the present work). Size-dependent aerosol pro-
20 cesses are expressed by segregating the size distributions of sea-salt aerosols into 8 size bins according to their dry radius (from 0.06 µm to 16 µm). For each bin, volumetric mean values are prescribed for liquid water content, atmospheric residence time, and mass transfer coefficients of chemical species, based on methods described in Toyota et al. (2001). The size distributions of dry sea-salt aerosols are taken from Porter and
25 Clarke (1997), and linearly scaled to yield the total mass concentrations predicted by an empirical relationship between sea-salt mass loading and wind speed (Blanchard and Woodcock, 1980). In the present work model runs are conducted at the wind speed

of 9 m/s, which yields 16.4 µg/m^3 for the mass concentration of dry sea-salt aerosols. Actinic flux is calculated based on a two-stream algorithm in the pseudo-spherical atmosphere (Kylling, 1995; Kylling et al., 1995). It is assumed that the actinic flux inside aerosol particles is enhanced by a factor of two relative to that in the surrounding air as a result of multiple scattering within the particles (Ruggaber et al., 1997). Numerical integration is performed with the Livermore Solver for Ordinary Differential Equations with general Sparse jacobian matrix (LSODES) (Hindmarsh, 1983). Although actual time steps for integration are determined internally by LSODES depending on the stiffness of the ordinary differential equation system, the external time step is set to 120 seconds at which interval diurnally varying photolysis rates (J values) are given.

The mid-latitude remote MBL condition is assumed for all model runs: 40°N, Julian day 80 (equinox), 340 DU total ozone, clear sky, and the sea surface albedo of 0.05 for calculating actinic flux; 1013.25 hPa total pressure, 293 K temperature, and 76.2% relative humidity for calculating reaction rates and hygroscopic particle growth. O_3 mixing ratio is fixed at 20 nmol/mol (Johnson et al., 1990; Oltmans and Levy, 1994). The mixing ratios of relatively long-lived VOCs are also fixed at values typical of remote MBL: $[CH_4]$ = 1.7 µmol/mol, $[C_2H_6]$ = 400 pmol/mol, $[C_3H_8]$ = 18 pmol/mol, $[C_2H_2]$ = 35 pmol/mol, and [CO] = 80 nmol/mol (Gregory et al., 1996); $[CH_3COCH_3]$ = 400 pmol/mol (Singh et al., 2001); $[CHBr_3]$ = 1 pmol/mol (Penkett et al., 1985; Yokouchi et al., 1997).

For shorter-lived species such as alkenes, nitrogen oxides, and DMS, influxes from the ocean surface and/or from the free troposphere are invoked to maintain their calculated mixing ratios in the MBL (see Table 2). The oceanic emissions of C_2H_4 and C_3H_6 are taken from five independent works, which derived different values by more than an order of magnitude (Donahue and Prinn, 1990; Bonsang, 1993; Plass-Dülmer et al., 1993; Thompson et al., 1993; Heikes et al., 1996). Oceanic CH_3CHO emissions are estimated so as to give the observed mixing ratios in the remote MBL (Singh et al., 2001; Wisthaler et al., 2002). NO_y is supplied into the model box in the form of NO, NO_2, HNO_3, or PAN by entrainment from the free troposphere (1.5×10^9 molecule cm^{-2} s^{-1})

and by emission from the ocean (7×10^7 molecule cm^{-2} s^{-1}). A large fraction of NO, NO$_2$, and PAN will be converted to HNO$_3$ or BrONO$_2$ via photochemical processes in the MBL, thereby serving as a source of NO$_3^-$ in the sea-salt aerosols along with HNO$_3$ entrained from the free troposphere. Similarly, DMS emitted from the ocean (2×10^9 molecule cm^{-2} s^{-1}) will be oxidized to give SO$_4^{2-}$ or CH$_3$SO$_3^-$. In our model runs NO$_3^-$, SO$_4^{2-}$, and CH$_3$SO$_3^-$ thus produced are the principal sources of acidity in sea-salt aerosols (see Figs. 3d-f). Among the species emitted from the ocean, NO, C$_2$H$_4$, C$_3$H$_6$, and CH$_3$CHO are primarily produced via photochemical processes in seawater (Zafiriou and McFarland, 1981; Ratte et al., 1993, 1998; Zhou and Mopper, 1997) and hence their emission rates are scaled by diurnally varying J(NO$_2$) values.

Organic oxygenates, whether halogenated or not, will be subject to dry and/or wet deposition. In the present work dry deposition velocities for organic oxygenates are given as follows: 0.1 cm/sec for ketones and alcohols, 0.5 cm/sec for peroxy radicals, hydroperoxides, aldehydes except for CH$_3$CHO, and carbonyl halides (e.g. HCOBr), and 1 cm/sec for carboxylic acids. The dry deposition velocities (v_0) are then converted to first-order loss rate coefficients (D) in the model box following an approach taken by Levy et al. (1985):

$$D = \frac{v_0}{Z_{mbl}} \frac{1}{1 + v_0/C_M U_s}$$

where Z_{mbl} is the MBL thickness (= 1 km), C_M is bulk coefficient for mass transfer over the ocean (= 0.0011; Garratt, 1992), and U_s is wind speed over the ocean (= 9 m/s). The wet deposition is assumed to take place for carboxylic acids, aldehydes, and carbonyl halides as a first-order loss process with τ = 8 day.

5. Results and Discussion

In the present work the impacts of acetaldehyde, alkenes, and acetylene on bromine activation are assessed by varying their oceanic emission rates or their mixing ratios

Title Page

Abstract | Introduction

Conclusions | References

Tables | Figures

◄◄ | ►►

◄ | ►

Back | Close

Full Screen / Esc

Print Version

Interactive Discussion

in the MBL (see Table 3). In each run numerical integration is carried out for 20 days long, starting at 0:00 a.m. local sun time. Initially, halogen species are present only in the forms of Br^- (~ 9.8 pmol/mol) and Cl^- (~ 6.4 nmol/mol) within nascent sea-salt aerosols, HCl (60 pmol/mol) and $CHBr_3$ (1 pmol/mol) in the gas phase. Uptake

5 of sulfur and nitrogen oxides from the gas phase initiates radical chain reactions in the deliquesced sea-salt aerosols, which consequently release a small amount of Br_2 to the gas phase. At the same time sea-salt aerosols other than those belonging to the largest-size bin are acidified and buffered to pH of about 4-5 by releasing (or scavenging) HCl to (or from) the gas phase (see Figs. 3a-f). Under sunlight Reactions (1)–(10)

10 also operate to release Br_2 and BrCl from the acidified sea-salt aerosols and thus the amounts of reactive halogen species increase appreciably with time (see Figs. 4a-f). Within 10 days or so, the temporal evolutions of pH and Cl^- deficits in the sea-salt aerosols other than those belonging to smallest-size bins are getting stabilized and the buildup of reactive halogens is limited by the decreased availability of Br^- in the sea-

15 salt aerosols. However, pH and Cl^- deficits in the sea-salt aerosols of smallest-size bins evolve slowly with time in accordance with the accumulation of sulfate until Day 20. This causes the gradual buildup of reactive halogens lasting until Day 20.

In Runs 1a-e and 2-6, the oceanic emission rate(s) of either CH_3CHO or alkenes are varied to examine their impacts on reactive halogen chemistry. Here the mixing

20 ratios of HCHO, CH_3CHO, C_2H_4, and C_3H_6 are calculated according to their oceanic emissions, photochemical sources/sinks, and dry/wet deposition to the sea surface with the initial mixing ratios given as $[C_2H_4] = [C_3H_6] = 0$ pmol/mol, $[CH_3CHO] = 90$ pmol/mol, and $[HCHO] = 300$ pmol/mol in each run. Their mixing ratios generally reach quasi-steady states on shorter time scales than those of reactive halogens (not

25 shown). Thus the quasi-steady-state levels of reactive halogens after Day 10 and their transient behaviors before that are persistently affected by the "adjusted" mixing ratios of these alkenes and aldehydes. Before proceeding to discussion about their influence on halogen chemistry, we will describe how the simulated mixing ratios of alkenes and aldehydes are related to their oceanic emissions.

Title Page

Abstract | Introduction

Conclusions | References

Tables | Figures

◄◄ | ►►

◄ | ►

Back | Close

Full Screen / Esc

Print Version

Interactive Discussion

5.1. Impacts of oceanic emissions on the mixing ratios of C_2H_4, C_3H_6, CH_3CHO, and HCHO

First of all, it should be noted that halogen chemistry plays a minor role in the photochemical loss of C_2H_4, C_3H_6, HCHO, and CH_3CHO in the MBL. Breakdowns of their photochemical loss processes simulated in Run 1a (base run) are as follows: for C_2H_4 90% by OH attack, 9% by reaction with O_3, and the remaining 1% by reactions with halogen atoms (mainly Cl atoms); for C_3H_6 83% by OH attack, 14% by reaction with O_3, and the remaining 3% by reactions with halogen atoms (mainly Br atoms); for HCHO 64% by photolysis, 35% by OH attack, and 1% by reactions with halogen atoms (mainly Br atoms); for CH_3CHO 90% by OH attack, 5% by photolysis, and 5% by reactions with halogen atoms (mostly Br atoms). NO_3 attacks in the gas phase and aqueous-phase loss processes within deliquesced sea-salt aerosols make negligible contributions to the loss of HCHO and CH_3CHO. Thus, the changing level of activity in halogen chemistry as will be demonstrated in the following sections is not a critical factor for determining the mixing ratios of these alkenes and aldehydes.

The oceanic emissions of alkenes and their resultant buildup in the MBL, if they are large enough, can appreciably augment the photochemical loss rate of OH radicals (Donahue and Prinn, 1990). In our model runs, however, the simulated concentrations of OH radical, which is the most important scavenger of alkenes, change by not more than 25% following more than an order of magnitude change in oceanic alkene fluxes (see Table 4). In addition, the mixing ratio of O_3, which is the second most important scavenger of alkenes, is fixed at the same value (20 nmol/mol) in all model runs. Thus, the simulated mixing ratios of alkenes are virtually linearly related to their oceanic emission rates. Among the model runs conducted, Run 1a takes the alkene emission rates from Bonsang (1993) and then yields 89.9 pmol/mol of C_2H_4 and 12.6 pmol/mol of C_3H_6 on Day 20. The mixing ratios of C_2H_4 and C_3H_6 simulated in Runs 1a are near the upper end and in the middle range, respectively, of those observed in the MBL (see Table 1). On the other hand, Run 5 takes the alkene emission rates from Thompson

Title Page

Abstract | Introduction

Conclusions | References

Tables | Figures

◄ | ►

◄ | ►

Back | Close

Full Screen / Esc

Print Version

Interactive Discussion

et al. ([1993](#)) and then yields 29.9 pmol/mol of C_2H_4 and 5.4 pmol/mol of C_3H_6 on Day 20, somewhat lower than those obtained in Run 1a. In this case, the simulated mixing ratio of C_2H_4 is in the middle range of the observed data, whereas that of C_3H_6 is rather in the lower range of the observed data. Since C_3H_6 exerts a much stronger influence on halogen chemistry than C_2H_4 does within these ranges of mixing ratios (see Sects. [5.3](#)–[5.4](#)), Run 1a is regarded as a base run in the present work. Where the alkene emission rates are taken from Plass-Dülmer et al. ([1993](#)) (Run 3) or from Heikes et al. ([1996](#)) (Run 4), the mixing ratios of C_2H_4 and C_3H_6 are calculated to be lower than 14 pmol/mol and 4 pmol/mol, respectively, which are near the lower ends of observed values. Finally, Run 6 takes the alkene emission rates from Donahue and Prinn ([1990](#)) and yields approximately 330 pmol/mol of C_2H_4 and 130 pmol/mol of C_3H_6 on Day 20. Although these mixing ratios are well above the values typically observed in the MBL remote from continental influences, a resultant influence on bromine chemistry is noteworthy as will be shown in Sect. [5.3](#). Since alkenes higher than C_3H_6 (isoprene in particular) are also emitted from the ocean (Donahue and Prinn, 1993; Pszenny et al., 1999; Yokouchi et al., 1999; Baker et al., 2000) and then react quite rapidly with Br atoms (Bierbach et al., 1996), Run 6 can be regarded as mimicking a potentially feasible situation in which such higher alkenes play important roles.

In the case of aldehydes, relationships between oceanic emissions and simulated mixing ratios are relatively complicated due to the presence of their secondary formation via photochemical processes. In Run 1a, in which the oceanic emission rate of CH_3CHO is set to 3.6×10^9 molecule cm^{-2} s^{-1}, CH_3CHO mixing ratio is calculated to be approximately 95 pmol/mol. This mixing ratio matches quite well with those observed by Singh et al. ([2001](#)) in the tropical/subtropical Pacific MBL (see Table [1](#)). Where the oceanic emission of CH_3CHO is switched off (Run 1b), its simulated mixing ratio is decreased to as low as 11.6 pmol/mol, implying that a significant amount of CH_3CHO originates from the oceanic emission in the remote MBL. In this run about half of CH_3CHO originates from C_2H_6 degradation and the remaining half from C_3H_6 degradation. Thus, the oceanic CH_3CHO emission rate being 2.2 times larger than that

in Run 1a, i.e. 8×10^9 molecule cm^{-2} s^{-1}, is sufficient to reproduce more than twice as high as CH$_3$CHO mixing ratio as observed by Wisthaler et al. (2002) in the equatorial Indian Ocean (Run 1c; see Tables 1 and 4). It is interesting to note that C$_3$H$_6$, if present as abundant as in Run 6, can also provide a dominant source of CH$_3$CHO.

5   The range of HCHO mixing ratios simulated in our model runs (260.8–406.7 pmol/mol; see Table 4) matches fairly well with those observed at Cape Grim (ca. 250–450 pmol/mol; Ayers et al., 1997), in the tropical Atlantic MBL south of ITCZ (~300–700 pmol/mol; Junkermann and Stockwell, 1999), and in the tropical Pacific MBL (~300 pmol/mol; Singh et al., 2001). Although CH$_4$ oxidation provides a domi-
10   nant source of HCHO in our model runs, the simulated mixing ratio of HCHO shows some dependence on alkene emission rates from the ocean. Both C$_2$H$_4$ and C$_3$H$_6$ are the precursors of HCHO and thus augment its production rate in the MBL. In addition to such a direct influence, alkene emissions from the ocean influence the simulated HCHO mixing ratio indirectly by modifying NO$_x$ abundance via bromine chemistry. As
15   will be shown in Sect. 5.3, bromine chemistry will be less activated at higher alkene mixing ratios Then, NO$_x$ mixing ratio is increased at lower levels of BrO, since Reaction (10) and subsequent aerosol uptake of BrONO$_2$ represent an efficient oxidation pathway of NO$_2$ in the MBL (Sander et al., 1999; Toyota et al., 2001). As NO$_x$ mixing ratio is increased, the yield of HCHO from CH$_4$ oxidation is also increased and
20   the yield of CH$_3$OOH is decreased instead (see Table 4). On the same grounds, the oceanic emission of CH$_3$CHO exerts an indirect influence on the simulated mixing ratio of HCHO (and CH$_3$CHO itself) by modifying NO$_x$ levels via bromine chemistry.

5.2.   Impacts of CH$_3$CHO emission on bromine chemistry

Figure 4a shows the temporal evolution of bromine species in Run 1a (base run), in
25   which quasi-steady-state mixing ratios of C$_2$H$_4$, C$_3$H$_6$, HCHO, and CH$_3$CHO simulated on Day 20 are 89.9, 12.6, 301.2, 94.7 pmol/mol, respectively. The total mixing ratio of inorganic gaseous bromine species, which originate mostly from volatilization from sea-

salt aerosols with a small contribution (∼3.7%) from $CHBr_3$ degradation (see Fig. 5), reaches about 5.2 pmol/mol on Day 20. This mixing ratio matches fairly well with those observed by Rahn et al. (1976) at Bermuda and by Rancher and Kritz (1980) in the MBL off the west African coast (see Sect. 1). By analyzing aerosol samples obtained simultaneously with the gas samples reported in the latter literature, Kritz and Rancher (1980) determined the concentration of particulate bromine and its fractional deficit relative to seawater (assuming that all aerosol particles consist of sea-salt aerosols) to be approximately 5 pmol/mol and 32%, respectively, on average. Again, these values are fairly close to those obtained in Run 1a: 6.1 pmol/mol of Br^- in sea-salt aerosols and 37.5% of Br^- deficit on Day 20. An appreciable amount of organic gaseous bromine species is also formed via Br-initiated degradation of C_2H_4, C_3H_6, and C_2H_2, building up along with inorganic gaseous bromine species (see Sect. 5.3 for further discussion).

As noted before, reactions converting Br atoms to HBr are capable of regulating bromine chemistry in the MBL by impeding the autocatalytic halogen release. On the Day 20 of Run 1a, the conversion of Br atoms to HBr occurs at the rate of 14.0 pmol/mol/day (see Fig. 5), of which 6.5 pmol/mol/day happens via Reaction (14) and 7.0 pmol/mol/day via Reaction (15). Thus, virtually half of HBr formation originates from the reaction between Br atoms and CH_3CHO in Run 1a. Such a substantial contribution from CH_3CHO is mainly due to the fact that CH_3CHO is 3.4 times (at 293 K) more reactive toward Br atoms than HCHO is (see rate constants for G53 and G84 in Table S1 in the electronic supplement, http://www.atmos-chem-phys.org/ acpd/3/4549/acpd-3-4549_supp.zip). On a daily average basis the mixing ratio of HBr thus produced reaches 2 pmol/mol, making up about 38% of the total mixing ratio of inorganic gaseous bromine species. It appears that a significant fraction of bromine volatilized from sea-salt aerosols is sequestered as HBr thereby making the availability of HOBr and $BrONO_2$ lower. In particular, HBr constitutes nearly 70% of inorganic gaseous bromine during the daytime when Reactions (1)–(10) operate to release reactive halogen species from sea-salt aerosols (see Fig. 6a). It is also interesting to note that about 90% of HBr participates again in the reaction sequence of autocatalytic

halogen release via either aqueous-phase reactions in the sea-salt aerosols or OH attack in the gas phase, whereas only 10% is irreversibly lost by dry/wet deposition (see Fig. 5).

⁵ In order to demonstrate further the importance of CH_3CHO for bromine chemistry in the remote MBL, two sensitivity runs are conducted in which the oceanic emission of CH_3CHO is either neglected (Run 1b) or increased by a factor of about 2.2 (Run 1c). In Run 1b CH_3CHO mixing ratio reaches as low as 12 pmol/mol, which is lower by 83 pmol/mol than that in Run 1a. HCHO mixing ratio is also decreased by 40 pmol/mol as a result of the secondary effect mediated by bromine chemistry (see Sect. 5.1). It fol-
¹⁰ lows that the conversion of Br atoms into HBr occurs in Run 1b almost half as frequently as it does in Run 1a and that the partitioning of HBr in inorganic gaseous bromine is decreased in Run 1b accordingly (see Fig. 6b). Consequently, bromine chemistry is activated more and the total amount of inorganic gaseous bromine species that build up on Day 20 is 2.8 times greater than that in Run 1a (see Fig. 4b and Table 4). The
¹⁵ reverse situation takes place in Run 1c. The CH_3CHO mixing ratio reaches as high as 210 pmol/mol and the HCHO mixing ratio is increased by 30 pmol/mol as a result of the secondary effect; consequently, the conversion frequency of Br atoms into HBr is nearly doubled compared with that in Run 1a. Then the total amount of inorganic gaseous bromine species that build up on Day 20 is only 42% of that in Run 1a (see
²⁰ Fig. 4c and Table 4).

The temporal and spatial variabilities in the sea-air flux of CH_3CHO and in its concentration in the MBL are not well characterized at the present time; however, recent observations suggest that CH_3CHO mixing ratio in the remote MBL can vary from less than 70 pmol/mol to over 250 pmol/mol (Singh et al., 2001; Wisthaler et al., 2002).
²⁵ From the results presented here, we would expect that a natural variability in atmospheric CH_3CHO mixing ratio represents an important factor for regulating bromine chemistry in the remote MBL (see also Sect. 5.4).

Although the rate constant for Reaction (16) is even greater than that for Reaction (15), the mixing ratios of C_2H_5CHO (formed exclusively from C_3H_8 oxidation) are cal-

Photochemistry of VOCs and halogens in the MBL

K. Toyota et al.

© EGU 2003

culated to be not more than 0.2 pmol/mol in our model runs. Therefore it is tentatively concluded that C_2H_5CHO is of negligible importance for bromine chemistry in the remote MBL. There might be a possibility, however, that a substantial amount of C_2H_5CHO is emitted from the ocean along with CH_3CHO and then affects bromine

5   chemistry in the MBL. It should also be noted that chemistry of $1\text{-}C_4H_8$, which provides a source for C_2H_5CHO, is neglected in the present work. An appreciable amount of $1\text{-}C_4H_8$, although slightly smaller than that of C_3H_6, is likely to be emitted from the ocean (Bonsang, 1993; Plass-Dülmer et al., 1993). Since alkyl aldehydes tend to be more reactive toward Br atoms as the carbon number of alkyl group increases (Ramacher

10   et al., 2000), measurements of C_2H_5CHO and still higher alkyl aldehydes in the MBL and in seawater would deserve consideration.

5.3.   Impacts of alkene emissions on bromine chemistry

As shown in Figs. 4a-f and Table 4, organic gaseous bromine species are formed photochemically in the presence of alkenes and C_2H_2, building up along with inor-

15   ganic gaseous bromine species. In Run 1a (base run), the total mixing ratio of organic gaseous bromine species that are formed from Br-initiated degradation of alkenes and C_2H_2 (i.e. excluding $CHBr_3$ and its degradation product CBr_2O; hereafter the terms "organic gaseous bromine species" and "brominated organic intermediates" refer to those produced via Br-initiated degradation of alkenes and C_2H_2) reaches approxi-

20   mately 30% of that of inorganic gaseous bromine species. These brominated organic intermediates consist mainly of hydroperoxides and carbonyl compounds (see Fig. 7). The three main brominated hydroperoxides, i.e. $CH_3CH(OOH)CH_2Br$, $BrCH_2OOH$, and $BrCH_2CH_2OOH$, collectively constitute 58% of the total amount of brominated organic intermediates in Run 1a. The predominance of hydroperoxides over carbonyl com-

25   pounds is due to our experimental conditions representing the low-NO_x environment. Appreciable amounts of brominated carboxylic acids, percarboxylic acids, and alcohols are also formed. In the present work brominated carboxylic acids ($BrCH_2COOH$ and $CH_3CHBrCOOH$) are allowed to be dissolved in deliquesced sea-salt aerosols (see Ta-

bles S4-5); however, they reside mostly in the gas phase and do not make noticeable contributions to bromine content in the sea-salt aerosols.

It should be noted that Br-initiated C_2H_2 degradation makes a negligible contribution to the formation of brominated organic intermediates. In run 2, in which the oceanic emissions of alkenes are neglected, HCOBr formed via Reaction (69) solely makes up the brominated organic intermediate and its mixing ratio reaches only 0.007% of the total mixing ratio of inorganic gaseous bromine species (see Table 4 and Fig. 4d; see also discussion in Sect. 5.5). Accordingly, the simulated molar ratio of the total amount of organic gaseous bromine species to that of inorganic counterparts (o-Br_x/i-Br_x ratio) depends strongly on the mixing ratios of alkenes in our model runs. In Run 3, in which the simulated mixing ratios of alkenes are an order of magnitude lower than those in Run 1a, o-Br_x/i-Br_x ratio (~0.034) also becomes lower by an order of magnitude than that in Run 1a (~0.30). On the other hand, the simulated mixing ratios of C_2H_4 and C_3H_6 in Run 6 are 3.7 times and 10.7 times, respectively, higher than those in Run 1a. In this case, organic gaseous bromine species become more abundant than inorganic counterparts and the o-Br_x/i-Br_x ratio of as high as 1.86 is obtained (see Table 4 and Fig. 4f). It should also be noted that C_3H_6 makes a larger contribution to the formation of brominated organic intermediates than C_2H_4 does in our model runs, primarily because C_3H_6 is approximately 20 times more reactive toward Br atoms than C_2H_4 is. This is demonstrated in sensitivity runs for Run 1a in which either C_2H_4 emission or C_3H_6 emission is neglected. In the former case (Run 1d), the simulated o-Br_x/i-Br_x ratio still reaches ~0.21. In the latter case (Run 1e), however, the simulated o-Br_x/i-Br_x ratio reaches only ~0.087, even though the mixing ratio of C_2H_4 (~88 pmol/mol) is near the upper end of observed values. Finally, as noted in Sect. 5.1, alkene mixing ratios simulated in Runs 1a-c and 5 most likely represent typical values observed in the remote MBL. The simulated o-Br_x/i-Br_x ratios in these runs range from 0.13 (Run 5) to 0.41 (Run 1b). Thus, the total mixing ratio of organic gaseous bromine species is likely to reach 10–20% or more of that of inorganic counterparts over wide regions in the MBL.

To sum up, an appreciable amount of reactive inorganic bromine species is converted to and sequestered as relatively inactive organic forms via reactions between alkenes and Br atoms. It follows that the oceanic emissions of alkenes, as with CH_3CHO, impede bromine activation in the MBL. Where the oceanic emissions of both C_2H_4 and C_3H_6 are neglected (Run 2), the total mixing ratio of inorganic gaseous bromine species on Day 20 reaches 10.9 pmol/mol, which is approximately twice as high as that in Run 1a (see Table 4 and Fig. 4d). Even in Runs 3 and 4, where the simulated mixing ratios of C_2H_4 and C_3H_6 are near the lower ends of observed values, the amounts of inorganic gaseous bromine species that build up on Day 20 are decreased by 9% and 20%, respectively, compared with that in Run 2 (see Table 4). In an extreme situation where the simulated mixing ratios of alkenes both exceed 100 pmol/mol (Run 6), the amount of inorganic gaseous bromine species that build up on Day 20 is an order of magnitude smaller than that in Run 2 (see Table 4 and Fig. 4f). It is interesting to note that the conversion of Br atoms into brominated organic intermediates via reactions with alkenes occurs at a rate more than an order of magnitude slower than the conversion of Br atoms into HBr via reactions with aldehydes in Run 1a (see Fig. 5). Once formed, however, brominated organic intermediates are fairly resistant to further degradation to regenerate inorganic bromine species. Their degradation to inorganic bromine occurs mostly via decomposition of brominated alkoxy radicals (Reactions (28)–(29)) and brominated acetyl radicals (Reaction (35)) and via heterogeneous reactions of HCOBr on the aerosol surface. By dividing the sum of the formation rates of Br atoms, HBr, and Br^- from brominated organic intermediates into their total concentration, an average time scale for brominated organic intermediates to regenerate inorganic bromine is estimated to be 57 hours. This time scale is much longer than that for the reentry of HBr into the reaction sequence of autocatalytic halogen release, i.e. Reactions (1)–(10), by aerosol uptake or via OH attack, which is estimated to be 3.7 hours. Thus, brominated organic intermediates are capable of building up to notable amounts, making the availability of reactive inorganic bromine species lower than would be without alkenes. Among the brominated organic intermediates thus pro-

duced, about 59% regenerates inorganic bromine species and the remainder is subject to dry/wet deposition in Run 1a. Consequently, the dry/wet deposition of brominated organic intermediates makes up 22% of the total deposition of bromine on Day 20.

Based largely on estimated rate constants, predictions made in the present work should be subject to errors associated with such estimates. In particular, the rate constants of OH-attacks/photolysis of brominated hydroperoxides exclusively rely on estimation, even though they constitute more than half of brominated organic intermediates (see Fig. 7). Table 5 presents the budgets of three main brominated hydroperoxides formed in Run 1a. It is estimated that the photochemical loss of these hydroperoxides are generally dominated by OH attacks with an order of magnitude smaller contribution from photolysis and that estimated photochemical lifetimes do not differ much among these hydroperoxides (22–36 hours). As described in Sect. 3.6, the rate constants of OH attacks on brominated hydroperoxides are estimated based on the SAR method with relevant parameters taken from Kwok and Atkinson (1995), Jenkin et al. (1997), and Saunders et al. (2003). Kwok and Atkinson (1995) alerted that the extended use of the SAR method as applied in the present work is subject to errors in estimated rate constants by a factor of two or more. However, the errors as large as an order of magnitude would be quite unlikely to occur for the majority of reactions. Regarding the photolysis of brominated hydroperoxides, our estimation of their J value (being identical to that for CH_3OOH) is solely based on the experimental evidence that absorption cross sections of CH_3OOH and $HOCH_2OOH$ virtually coincide with each other (see Sect. 3.6). Therefore, a sensitivity run is performed in which absorption cross sections of brominated hydroperoxides are red-shifted by 50 nm relative to those of CH_3OOH (Run 1f). In this case, 24-hour average J value for brominated hydroperoxides is increased to $1.76 \times 10^{-5}\,\mathrm{s}^{-1}$, which is greater than that in the base run by a factor of 15. Then, photolysis becomes a major loss process for brominated hydroperoxides and their overall photochemical lifetimes are generally shortened by a factor of three or less. As a result, the mixing ratios of brominated hydroperoxides are decreased approximately by a factor of two (see Fig. 7). This accompanies a slight

increase in the mixing ratios of brominated carbonyl compounds and their degradation products including $BrCH_2OOH$, since the degradation of brominated hydroperoxides represents one of the important sources of brominated carbonyl compounds (see Table 6). Overall, an appreciable amount of organic brominated intermediates, reaching

5 1.1 pmol/mol (18% of that of inorganic gaseous bromine species), is still formed in Run 1f and the total mixing ratio of inorganic gaseous bromine species is simulated to be only 14% higher than that in Run 1a (see Table 4). In the remote MBL with low NO_x concentrations, a large fraction of alkenes that react with Br atoms forms brominated hydroperoxides, whose further degradation results in the formation of brominated

10 carbonyl compounds. Decomposition of brominated alkoxy/acetyl radicals, which are formed via further degradation of brominated carbonyl compounds, provides a main pathway to regenerate inorganic bromine (Br atoms) from brominated organic intermediates. Thus, the number of reaction steps to regenerate inorganic bromine species from brominated organic oxygenates are fairy large so that simulated results will not

15 be highly sensitive to errors in the rate estimates.

One may expect a possibility that halogenated hydroperoxides (and other halogenated organic oxygenates formed along with them) are decomposed more promptly than estimated in the present work to regenerate inorganic halogen species via some unknown mechanisms. In their modeling study concerning "bromine explosion" in the

20 Arctic boundary layer, McConnell et al. (1992) even assumed that brominated hydroperoxides and other brominated organic oxygenates are effectively scavenged on the surfaces of snow and aerosols and are then converted to Br_2 via reaction with Br^-:

$$\text{Organic-Br} + Br^- \rightarrow Br_2 + \text{products}. \tag{76}$$

However, the feasibility of such reactions has never been explored with laboratory ex-

25 periments. We would expect that such reactions, if they do happen, proceed very slowly as in the case of aqueous-phase reactions between PAA and Cl^-/Br^- and do not exert any noticeable influences on the behaviors of halogenated organic oxygenates (see Sect. 5.6). It should also be noted that wall reactions of $ClCH_2OOH$ and

BrCH$_2$OOH were unobservable in previous chamber experiments (Chen et al., 1995; Wallington et al., 1996).

In this respect, a reactive uptake coefficient (γ) as large as 0.1 is already assigned for the heterogeneous reaction of HCOBr to give HBr + CO in the base run (see Sect. 3.2). The rapid heterogeneous loss makes the chemical lifetime of HCOBr shorter than 3 hours and provides an important pathway to regenerate inorganic bromine from brominated organic intermediates (see Table 6 and Fig. 5). In a sensitivity run (Run 1g) with a decreased value of γ as low as 8×10^{-4} as in the case of heterogeneous reactions of acetyl halides, HCOBr mixing ratio becomes more than an order of magnitude higher than that in Run 1a (see Fig. 7). However, a change in the simulated mixing ratio of inorganic gaseous bromine species is less than 5% from Run 1a (see Table 4). This again suggests that the uncertainty in kinetic parameters for a single reaction does not represent a serious flaw in our model prediction.

5.4. Additional model runs with the fixed mixing ratios of HCHO/CH$_3$CHO/C$_2$H$_4$/C$_3$H$_6$

As described in the previous section, the oceanic alkene emissions impede bromine activation in the MBL by forming brominated organic intermediates ("direct" influence). Actually, the oceanic emissions of alkenes also result in the increase in the mixing ratios of CH$_3$CHO and HCHO in the MBL (see Sect. 5.1). This could represent an additional factor for impeding bromine activation ("indirect" influence). In order to separate contributions from the "direct" influence and those from the "indirect" influence, model runs are conducted in which the mixing ratios of C$_2$H$_4$, C$_3$H$_6$, HCHO, and CH$_3$CHO are specified rather than simulated in the model (Runs 7a-d; see Tables 3 and 7). Runs 7a and 7b are conducted with the mixing ratios of C$_2$H$_4$, C$_3$H$_6$, HCHO, and CH$_3$CHO being specified to those taken from the daily average values on Day 20 in Runs 2 and 1a, respectively. Accordingly, the total mixing ratios of inorganic gaseous bromine species simulated on Day 20 in Runs 7a (11.15 pmol/day) and 7b (5.26 pmol/mol) are very close to those in Runs 2 and 1a, respectively. In Run 7c the mixing ratios of C$_2$H$_4$

Print Version

Interactive Discussion

and C_3H_6 are fixed at 0 pmol/mol (the same as Run 7a), whereas those of HCHO and CH_3CHO are increased to 301.2 pmol/mol and 94.7 pmol/mol, respectively, to match with those in Run 7b. On the other hand, in Run 7d the mixing ratios of C_2H_4 and C_3H_6 are fixed at the same values as those in Run 7b, whereas the mixing ratios of HCHO and CH_3CHO are decreased to 265.6 pmol/mol and 80.2 pmol/mol, respectively, to match with those in Run 7a. Then the total mixing ratios of inorganic gaseous bromine species are simulated to be 7.87 pmol/mol and 6.75 pmol/mol in Runs 7c and 7d, respectively, implying that the increase in CH_3CHO and HCHO mixing ratios by secondary effects augments appreciably the impacts of oceanic alkene emissions on bromine chemistry.

To survey the dependence of bromine activation on each of CH_3CHO, C_2H_4, and C_3H_6 mixing ratios within their probable ranges encountered in the remote MBL (see Table 1), three sets of parameter sweep experiments are also performed. In each experiment multiple model runs are conducted, taking [HCHO] = 300 pmol/mol, [CH_3CHO] = 90 pmol/mol, [C_2H_4] = 30 pmol/mol, and [C_3H_6] = 15 pmol/mol as a base condition. Here sensitivities of model behaviors on either CH_3CHO mixing ratio (from 0 to 250 pmol/mol; Run 8a), C_2H_4 mixing ratio (from 0 to 100 pmol/mol; Run 8b), or C_3H_6 mixing ratio (from 0 to 30 pmol/mol; Run 8c) are examined. Under the base condition the total mixing ratio of inorganic gaseous bromine species are simulated to be 5.73 pmol/mol with the o-Br_x/i-Br_x ratio of 0.29. As shown in Figs. 8a and 8c, the degree of bromine activation depends quite strongly on variabilities in CH_3CHO and C_3H_6 mixing ratios. Within the probable range of CH_3CHO mixing ratios in the remote MBL (70–250 pmol/mol) the total mixing ratio of inorganic gaseous bromine species range between 1.9–7.2 pmol/mol with o-Br_x/i-Br_x ratio ranging between 0.20–0.31. Within the probable range of C_3H_6 mixing ratios in the remote MBL (2–30 pmol/mol), the total mixing ratio of inorganic gaseous bromine species range between 4.5–7.6 pmol/mol with o-Br_x/i-Br_x ratio ranging between 0.06–0.54. A variability in C_2H_4 mixing ratio has a weaker influence on bromine activation than those in CH_3CHO and C_3H_6 mixing ratios do. As C_2H_4 mixing ratio is increased from 5 to

Photochemistry of VOCs and halogens in the MBL

K. Toyota et al.

Title Page

Abstract	Introduction
Conclusions	References
Tables	Figures

◄◄   ►►

◄   ►

Back   Close

Full Screen / Esc

Print Version

Interactive Discussion

90 pmol/mol (sweeping the probable range in the remote MBL), the total mixing ratio of inorganic gaseous bromine species is only decreased from 5.9 to 5.3 pmol/mol (see Fig. 8b).

5.5. Impacts of C_2H_2 on bromine activation

5 In their modeling study Sander et al. (1997) found that C_2H_2 as well as C_2H_4 can effectively impede the "bromine explosion" in the springtime Arctic boundary layer, given that all the Br atoms reacting with C_2H_2 produce organically-bound bromine compound(s) (most likely HCOBr) and that the product(s) are completely inert against further degradation to regenerate inorganic bromine species.

10 As experimentally determined by Yarwood et al. (1991) and Ramacher et al. (2001), however, less than 20% of the reaction Br + C_2H_2 results in HCOBr formation, whereas the remainder gives inorganic bromine species such as HBr or Br atoms (see Reaction (69)). In addition, HCOBr is likely to hydrolyze rapidly on aerosol surface to give HBr (see Sect. 3.2). Thus, in our model runs, C_2H_2 exerts no more than a marginal influence on bromine activation. As C_2H_2 mixing ratio is increased from 35 pmol/mol (Run 1a) to 200 pmol/mol (Run 1h) to represent an air mass under a relatively strong continental influence (e.g. Koppmann et al., 1992), the total mixing ratio of inorganic gaseous bromine species calculated is decreased by only 1.3% (from 5.22 pmol/mol to 5.15 pmol/mol). Even where the reactive uptake coefficient of HCOBr hydrolysis on aerosol surface is reduced from 0.1 to 8×10^{-4}, the impact of C_2H_2 is still very small; in this case, the calculated total mixing ratio of inorganic gaseous bromine species is decreased by 1.8% (from 4.99 pmol/mol to 4.90 pmol/mol), as C_2H_2 mixing ratio is increased from 35 pmol/mol (Run 1g) to 200 pmol/mol (Run 1i).

5.6. PAA as a trigger of autocatalytic halogen release from sea-salt aerosols

25 PAA is formed primarily via OH-initiated CH_3CHO oxidation in the gas phase (Reactions (70)–(71)). This compound is potentially important for triggering the autocatalytic

halogen release from sea-salt aerosols, since it is capable of oxidizing halide ions in the aqueous phase (Fortnum et al., 1960). To our knowledge atmospheric concentrations of PAA in the MBL have never been reported in the literature; however, its production and loss kinetics in the gas- and aqueous-phases have been characterized fairly well by earlier experimental studies (see Sect. 3.7) and besides the concentration of its precursor, CH_3CHO, can be constrained by recent observations in the remote MBL (Singh et al., 2001; Wisthaler et al., 2002). In our model runs the calculated mixing ratio of PAA varies between 27 to 157 pmol/mol, depending on the mixing ratios of CH_3CHO and NO_x (see Table 4). Then aqueous-phase reactions of PAA considered in the present work (Reaction (73)–(75)) take place so slowly that the aqueous-phase concentrations of PAA in deliquesced sea-salt aerosols are virtually in Henry's law equilibrium with its gas-phase concentrations.

Table 8 presents the rates of reactive halogen production via reactions of potential importance for triggering the autocatalytic halogen release in Run 1a (base run), in which the mixing ratio of PAA is calculated to be approximately 80 pmol/mol. As in the cases of preceding modeling works by Sander and Crutzen (1996) and Vogt et al. (1996), reactions between Cl^-/Br^- and HSO_5^- and the self-reaction of Br_2^- are primarily important for triggering the autocatalytic halogen release. They are the consequences of radical chain reactions initiated by the uptake of either OH (during the daytime) or NO_3 (during the nighttime) from the gas phase. Photolysis of NO_3^- also results in the formation of OH radicals and thus augments the OH concentrations in the deliquesced sea-salt aerosols (von Glasow et al., 2002a). The next important process as a trigger of autocatalytic halogen release is $CHBr_3$ degradation in the gas phase. The production of Br atoms via $CHBr_3$ degradation results in the formation of HOBr and $BrONO_2$ by subsequent gas-phase reactions (8)–(10) and is thus capable of triggering autocatalytic halogen release. The oxidation of halides by PAA occurs at a rate comparable to that of Br^- oxidation by O_3, reaching no more than a few percent of the rates of $Br^-/Cl^- + HSO_5^-$ during the daytime. During the nighttime, however, radical-initiated reactions are less active than during the daytime and therefore the contributions from

the reactions involving PAA become relatively greater, reaching 24% of those from the radical-initiated primary processes. Thus, PAA can serve as one of the important chemical agents for triggering the autocatalytic halogen release in the remote MBL during the nighttime. During the daytime, its impact is swamped by other mechanisms including the radical chain reactions oxidizing halides in the sea-salt aerosols and the production of Br atoms via $CHBr_3$ degradation in the gas phase.

Measurements of PAA in the MBL are clearly needed to better assess its impact.

5.7.   Implications for chemistry of DMS, NO_x, and O_3

As demonstrated in Sects. 5.2–5.4, the oceanic emissions of CH_3CHO and alkenes will significantly impede the autocatalytic halogen release from sea-salt aerosols in the remote MBL. Accordingly, the simulated mixing ratios of reactive bromine species can differ by a factor of two or more with or without oceanic emissions of these compounds (see Table 4 and Fig. 4).

Figures 9a-b show diurnal variations in the simulated concentrations of BrO radicals and Cl atoms on Day 20 for Runs 1a-b and 2. Here, Run 1a is our base run which we believe represents a typical condition in the remote MBL concerning the mixing ratios of CH_3CHO and alkenes, Run 1b is a sensitivity run in which the oceanic emission of CH_3CHO is neglected, and Run 2 is another sensitivity run in which the oceanic emissions of alkenes are neglected. In Run 1a, the mixing ratio of BrO is generally below 1 pmol/mol, rising to 1.3 pmol/mol shortly after sunrise. This level of BrO would be difficult to detect in the ambient air by currently available measurement techniques (see Sect. 1). Where the oceanic emissions of alkenes are switched off (Run 2), BrO mixing ratio is calculated to be somewhat higher, ranging <1–3.4 pmol/mol during the daytime. Among the model runs conducted in the present work, Run 1b yield a result with the most activated bromine chemistry by neglecting the oceanic emission of CH_3CHO (see Table 4). In this run BrO mixing ratio ranges generally between 1-2 pmol/mol during the daytime, rising to 5.3 pmol/mol shortly after sunrise. Again, currently available measurement techniques would be difficult to detect these levels of BrO in the

Title Page

Abstract	Introduction
Conclusions	References
Tables	Figures

| ◄◄ | ►► |
| ◄ | ► |

| Back | Close |

Full Screen / Esc

Print Version

Interactive Discussion

ambient air except for a short duration in the early morning when BrO mixing ratio well exceeds 2 pmol/mol. Thus the validity of our model prediction would be rather difficult to be tested against field measurement data of BrO radicals obtained by currently available techniques. As for Cl atoms, their daytime concentrations in Runs 1a-b and 2 range between 10^3–10^4 molecule/cm^3, matching fairly well with values inferred from observed concentrations of hydrocarbons and/or halocarbons and their correlations in the remote MBL (Rudolph et al., 1996, 1997; Singh et al., 1996a,b; Wingenter et al., 1996, 1999).

Quite interestingly, the impacts of halogen (especially bromine) chemistry on the budgets of DMS, NO$_x$, and O$_3$ are still appreciable in Run 1a (see Table 4). As compared with Run 1j, which is one of the sensitivity runs for Run 1a with halogen chemistry being switched off, the simulated mixing ratio of DMS is decreased by 20%, reflecting an additional photochemical loss via reactions with BrO radicals and Cl atoms that constitutes 24% of the total loss (see also Fig. 10). Here the reactions of DMS with Br atoms and ClO radicals are not accounted for in our reaction scheme, since the former reaction does not result in H-abstraction from DMS at atmospheric temperatures (Ingham et al., 1999; Nakano et al., 2001) and the rate constant of the latter reaction is approximately 30 times smaller than that of the reaction BrO + DMS (Barnes et al., 1991). As for NO$_x$, its mixing ratio is also decreased by 22% in Run 1a compared with that in Run 1j owing to the enhanced loss of NO$_2$ via Reaction (10) followed by aerosol uptake. Then, by combined effects from enhanced photochemical loss via bromine chemistry and from decreased photochemical production at lower NO$_x$ concentrations (Sander et al., 1999; Toyota et al., 2001), the net chemical production rate of O$_3$ changes from −0.71 nmol/mol/day to −1.09 nmol/mol/day. Taking a time scale for the exchange of air mass in the MBL with that in the free troposphere to be 3–4 days following the work of Ayers and Galbally (1995), the difference in the net chemical production noted above would lead to the difference of 1.14–1.52 nmol/mol (5.7–7.6% of the absolute amount, i.e. 20 nmol/mol) in O$_3$ mixing ratio. In Runs 1b and 2 the impacts of halogen chemistry are of course larger: reactions with BrO radicals and Cl atoms constitute 57%

(Run 1b) and 43% (Run 2) of the overall photochemical loss of DMS (see Fig. 10); NO_x mixing ratios are decreased by 54% (Run 1b) and 41% (Run 2) as compared with that in Run 1j; and the net chemical loss of O_3 reaches as high as 1.79 nmol/mol/day and 1.46 nmol/mol/day in Runs 1b and 2, respectively (see Table 4).

5   These results suggest that CH_3CHO and alkenes of oceanic origin should be carefully treated in the modeling of reactive halogen chemistry involving sea-salt aerosols. Even with the typical mixing ratios of CH_3CHO and alkenes observed in the remote MBL, reactive halogen chemistry simulated will be significantly suppressed as compared with the situations where their oceanic emissions are neglected. Quite impor-
10   tantly, the impacts of halogen chemistry on DMS, NO_x, and O_3 budgets are still appreciable on such occasions. From the results presented in Sects. 5.2–5.4, we would expect that naturally occurring variabilities in the oceanic emissions of CH_3CHO and alkenes permit changes in the amount of reactive halogen species to be higher or lower than that in Run 1a by a factor of about two. Taken together, reactive halogen chemistry
15   is likely to mediate a link between the oceanic emissions of VOCs and the behaviors of compounds that are sensitive to halogen chemistry such as DMS, NO_x, and O_3 in the MBL.

6. Conclusions

In order to investigate photochemical interactions between reactive halogen species
20   and volatile organic compounds in the remote MBL, the reaction scheme of multiphase photochemical box model SEAMAC (size-SEgregated Aerosol model for Marine Air Chemistry) is updated to achieve a near-explicit description of oxidative degradation of up to C_3-hydrocarbons (CH_4, C_2H_6, C_3H_8, C_2H_4, C_3H_6, and C_2H_2) initiated by reactions with OH radicals, Cl- and Br-atoms, and O_3. A variety of halogenated organic
25   compounds will be formed following the reactions of halogen atoms with C_2H_4, C_3H_6, and C_2H_2. However, kinetic and mechanistic data concerning their further degradation by OH attacks and/or photolysis are lacking in the majority of cases and are therefore

estimated by empirical methods including structure-activity relationships. Model calculations with the new reaction scheme reveal important roles played by CH_3CHO and alkenes of oceanic origin in regulating bromine chemistry in the remote MBL.

The reaction with CH_3CHO is an important sink for Br atoms, thereby impeding the autocatalytic halogen halogen release from sea-salt aerosols. The activity of reactive halogen chemistry in the mid-latitude remote MBL is expected to vary by a factor of two or more as a result of natural variability in CH_3CHO mixing ratio. CH_3CHO in the MBL originates most likely from its emission from the ocean and additionally from photochemical oxidation of C_2H_6/C_3H_6.

The addition reactions Br + C_2H_4/C_3H_6 are also important for impeding autocatalytic halogen release from sea-salt aerosols by producing brominated organic intermediates which sequester bromine from reactive inorganic pool. The total amount of brominated organic intermediates thus produced is likely to reach 10–20% or more of that of inorganic gaseous bromine species over wide regions over the remote ocean. The increase in CH_3CHO and HCHO mixing ratios that accompanies the oceanic alkene emissions will augment their impacts on halogen chemistry. Some uncertainties arise in the dearth of kinetic and photochemical data concerning the production and loss of brominated organic intermediates. Experimental studies to determine currently-unknown kinetic parameters, including the rate constants of OH attacks on brominated organic oxygenates and those of the reactions of brominated organic peroxy radicals with NO, HO_2, and RO_2, would benefit a better assessment of the impacts of alkenes on reactive halogen chemistry in the MBL. In the remote MBL with low NO_x concentrations, however, regeneration of inorganic bromine species from brominated organic oxygenates generally involves multiple reaction steps, and so that the simulated results will not change significantly by errors in the rate estimates. To our knowledge, this is the first study of its kind addressing the impacts of C_3H_6 on halogen chemistry in the lower troposphere. C_3H_6 reacts with Br atoms approximately 20 times faster than C_2H_4 does, thereby strongly impeding the rate of autocatalytic halogen release from sea-salt aerosols. C_2H_2 also forms a brominated organic compound, i.e. HCOBr, via reaction

K. Toyota et al.

Title Page	
Abstract	Introduction
Conclusions	References
Tables	Figures
◄◄	►►
◄	►
Back	Close
Full Screen / Esc	
Print Version	
Interactive Discussion	

with Br atoms. Its impact, however, appears unimportant for overall bromine cycle in the remote MBL.

Peroxyacetic acid (PAA) formed via CH_3CHO degradation is proposed to be one of the important chemical agents for triggering autocatalytic halogen release from sea-salt aerosols. Although we believe that PAA mixing ratios (27–157 pmol/mol) are quite reasonably simulated in our model runs, measurements of PAA in the remote MBL are needed to better assess its impact.

To date, the impacts of their emissions have been discussed within the context of HO_x-NO_x chemistry and/or organic acids formation (e.g. Arlander et al., 1990; Donahue and Prinn, 1990; Singh et al., 2001). The present work suggests that the oceanic emissions of CH_3CHO/alkenes and resultant variations in their atmospheric concentrations are important for regulating reactive halogen chemistry in the MBL as well. Quite interestingly, the model runs conducted in the present work reveal that the concentrations of reactive halogen species are more sensitively influenced by the oceanic emissions of these VOCs than the concentration of OH radicals is. In a situation typical of the mid-latitude remote MBL, autocatalytic halogen release from sea salt is significantly impeded by the reactions of Br atoms with CH_3CHO and alkenes. However, halogen chemistry still exerts an appreciable influence on the budgets of DMS, NO_x, and O_3 on such occasions. This also implies that the behaviors of these compounds in the MBL can be controlled indirectly by the oceanic emissions of VOCs as mediated by reactive halogen chemistry involving sea-salt aerosols.

References

Arimoto, R., Duce, R. A., Ray, B. J., Hewitt, A. D., and Williams, J.: Trace elements in the atmosphere of American Samoa: Concentrations and deposition to the tropical south Pacific, J. Geophys. Res., 92, 8465–8479, 1987. 4552

5 Arimoto, R., Ray, B. J., Duce, R. A., Hewitt, A. D., Boldi, R., and Hudson, A.: Concentrations, sources, and fluxes of trace elements in the remote marine atmosphere of New Zealand, J. Geophys. Res., 95, 22,389–22,405, 1990. 4552

Arlander, D. W., Cronn, D. R., Farmer, J. C., Menzia, F. A., and Westberg, H. H.: Gaseous oxygenated hydrocarbons in the remote marine troposphere, J. Geophys. Res., 95, 16,391–
10 16,403, 1990. 4554, 4597

Atkinson, R.: A structure-activity relationship for the estimation of rate constants for the gas-phase reactions of OH radicals with organic compounds, Int. J. Chem. Kinet., 19, 799–828, 1987. 4572

Atkinson, R., Baulch, D. L., Cox, R. A., Hampson, R. F., Jr., Kerr, J. A., Rossi, M. J., and
15 Troe, J.: Evaluated Kinetic, Photochemical and Heterogeneous Data for Atmospheric Chemistry: Supplement V, IUPAC Subcommittee on Gas Kinetic Data Evaluation for Atmospheric Chemistry, J. Phys. Chem. Ref. Data, 26, 521–1011, 1997. 4557, 4573

Atkinson, R., Baulch, D. L., Cox, R. A., Hampson, R. F., Jr., Kerr, J. A., Rossi, M. J., and Troe, J.: Evaluated Kinetic and Photochemical Data for Atmospheric Chemistry, Organic
20 Species: Supplement VII, IUPAC Subcommittee on Gas Kinetic Data Evaluation for Atmospheric Chemistry, J. Phys. Chem. Ref. Data, 28, 191–393, 1999. 4557, 4559, 4569, 4573, 4574, 4624

Ayers, G. P. and Galbally, I. E.: A preliminary estimation of a boundary layer-free troposphere entrainment velocity at Cape Grim, in Baseline 92, (Eds.) Dick, A. L. and Fraser, P. J., pp.
25 10–15, Bureau of Meteorology, Australia, 1995. 4594

Ayers, G. P., Gillett, R. W., Granek, H., de Serves, C., and Cox, R. A.: Formaldehyde production in clean marine air, Geophys. Res. Lett., 24, 401–404, 1997. 4581

Ayers, G. P., Gillett, R. W., Cainey, J. M., and Dick, A. L.: Chloride and bromide loss from sea-salt particles in Southern Ocean air, J. Atmos. Chem., 33, 299–319, 1999. 4552

30 Baboukas, E. D., Kanakidou, M., and Mihalopoulos, N., Carboxylic acids in gas and particulate phase above the Atlantic Ocean, J. Geophys. Res., 105, 14,459–14,471, 2000. 4554

Bacher, C., Tyndall, G. S., and Orlando, J. J.: The atmospheric chemistry of glycolaldehyde, J.

Title Page

Abstract | Introduction

Conclusions | References

Tables | Figures

◄◄ | ►►

◄ | ►

Back | Close

Full Screen / Esc

Print Version

Interactive Discussion

Atmos. Chem., 39, 171–189, 2001. 4624

Baker, A. R., Turner, S. M., Broadgate, W. J., Thompson, A., McFiggans, G. B., Vesperini, O., Nightingale, P. D., Liss, P. S., and Jickells, T. D.: Distribution and sea-air fluxes of biogenic trace gases in the eastern Atlantic Ocean, Global Biogeochem. Cycles, 14, 871–886, 2000. 4580

Barnes, I., Bastian, V., Becker, K. H., Overath, R., and Zhu, T.: Rate constants for the reactions of Br atoms with a series of alkanes, alkenes, and alkynes in the presence of O_2, Int. J. Chem. Kinet., 21, 499–517, 1989. 4557, 4562, 4564, 4566, 4569

Barnes, I., Bastian, V., Becker, K. H., and Overath, R. D.: Kinetic studies of the reactions of IO, BrO, and ClO with dimethylsulfide, Int. J. Chem. Kinet., 23, 579–591, 1991. 4594

Bauerle, S. and Moortgat, G. K.: Absorption cross-sections of $HOCH_2OOH$ vapor between 205 and 360 nm at 298 K, Chem. Phys. Lett., 309, 43–48, 1999. 4573, 4624

Bedjanian, Y., Poulet, G., and Le Bras, G.: Low-pressure study of the reactions of Br atoms with alkenes. 1. Reactions with propene, J. Phys. Chem. A, 102, 5867–5875, 1998. 4567

Bedjanian, Y., Poulet, G., and Le Bras, G.: Low-pressure study of the reactions of Br atoms with alkenes. 2. Reactions with ethene and *trans*-2-butene, J. Phys. Chem. A, 103, 4026–4033, 1999. 4560

Bierbach, A., Barnes, I., and Becker, K. H.: Rate coefficients for the gas-phase reactions of bromine radicals with a series of alkenes, dienes, and aromatic hydrocarbons at 298 ± 2 K, Int. J. Chem. Kinet., 28, 565–577, 1996. 4557, 4580

Bierbach, A., Barnes, I., and Becker, K. H.: FT-IR product study of the gas-phase Br-initiated oxidation of *trans*-2-butene under atmospheric conditions between 246 and 298 K, Tellus, 49B, 566–582, 1997. 4557, 4568

Bilde, M., Wallington, T. J., Ferronato, C., Orlando, J J., Tyndall, G. S., Estupiñan, E., and Haberkorn, S.: Atmospheric chemistry of CH_2BrCl, $CHBrCl_2$, $CHBr_2Cl$, $CF_3CHBrCl$, and CBr_2Cl_2, J. Phys. Chem. A, 102, 1976–1986, 1998. 4561

Bilde, M., Orlando, J J., Tyndall, G. S., Wallington, T. J., Hurley, M. D., and Kaiser, E. W.: FT-IR product studies of the Cl-initiated oxidation of CH_3Cl in the presence of NO, J. Phys. Chem. A, 103, 3963–3968, 1999. 4562

Blanchard, D. C. and Woodcock, A. H.: The production, concentration, and vertical distribution of the sea-salt aerosol, Ann. N. Y. Acad. Sci., 338, 330–347, 1980. 4575

Bonsang, B.: Hydrocarbons emission from the ocean, in The Tropospheric Chemistry of Ozone in the Polar Regions, NATO ASI Series I7, (Eds.) Niki, H. and Becker, K. H., pp. 251–260,

Springer-Verlag, Berlin, 1993. 4557, 4576, 4579, 4584, 4612, 4613, 4623

Bonsang, B., Kanakidou, M., Lambert, G., and Monfray, P.: The marine source of C_2-C_6 aliphatic hydrocarbons, J. Atmos. Chem., 6, 3–20, 1988. 4555, 4623

Burkholder, J. B., Gilles, M. K., Gierczak, T, and Ravishankara, A. R.: The atmospheric degradation of 1-bromopropane ($CH_3CH_2CH_2Br$): The photochemistry of bromoacetone, Geophys. Res. Lett., 29(17), 1822, doi:10.1029/2002GL014712, 2002. 4568, 4573, 4624

Carver, G. D., Brown, P. D., and Wild, O.: The ASAD atmospheric chemistry integration package and chemical reaction database, Comp. Phys. Comm., 105, 197–215, 1997. 4575

Chand, D., Lal, S., and Naja, M.: Variations of ozone in the marine boundary layer over the Arabian Sea and the Indian Ocean during the 1998 and 1999 INDOEX campaigns, J. Geophys. Res., 108(D6), 4190, doi:10.1029/2001JD001589, 2003. 4551

Chen, J., Catoire, V., and Niki, H.: Mechanistic study of the $BrCH_2O$ radical degradation in 700 Torr air, Chem. Phys. Lett., 245, 519–528, 1995. 4562, 4563, 4565, 4589

Chen, J., Young, V., Catoire, V., and Niki, H.: FTIR spectroscopic studies of the mechanisms of the halogen atom initiated oxidation of haloacetaldehydes, J. Phys. Chem., 100, 6580–6586, 1996. 4564

Chin, M., Rood, R. B., Allen, D. J., Andreae, M. O., Thompson, A. M., Lin, S. -J., Atlas, R. M., and Ardizzone, J. V.: Processes controlling dimethylsulfide over the ocean: Case studies using a 3-D model driven by assimilated meteorological fields, J. Geophys. Res., 103, 8341–8353, 1998. 4551

Crowley, J. N. and Moortgat, G. K.: 2-Bromoethylperoxy and 2-bromo-1-methylpropylperoxy radicals: Ultraviolet absorption spectra and self-reaction rate constants at 298 K, J. Chem. Soc. Faraday Trans., 88, 2437–2444, 1992. 4561

DeMore, W. B., Sander, S. P., Golden, D. M., Hampson, R. F., Kurylo, M. J., Howard, C. J., Ravishankara, A. R., Kolb, C. E., and Molina, M. J.: Chemical Kinetics and Photochemical Data for Use in Stratospheric Modeling, Evaluation 12, JPL Publication 97-4, Jet Propulsion Laboratory, Pasadena, California, 1997. 4557

Dickerson, R. R., Rhoads, K. P., Carsey, T. P., Oltmans, S. J., Burrows, J. P., and Crutzen, P. J.: Ozone in the remote marine boundary layer: A possible role for halogens, J. Geophys. Res., 104, 21,385–21,395, 1999. 4551, 4570

Donahue, N. M. and Prinn, R. G.: Nonmethane hydrocarbon chemistry in the remote marine boundary layer, J. Geophys. Res., 95, 18,387–18,411, 1990. 4554, 4556, 4557, 4576, 4579, 4580, 4597, 4612, 4613, 4623

Photochemistry of VOCs and halogens in the MBL

K. Toyota et al.

Title Page

Abstract	Introduction
Conclusions	References
Tables	Figures

◄◄   ►►

◄   ►

Back   Close

Full Screen / Esc

Print Version

Interactive Discussion

© EGU 2003

Donahue, N. M. and Prinn, R. G.: In situ nonmethane hydrocarbon measurements on SAGA 3, J. Geophys. Res., 98, 16,915–16,932, 1993. 4554, 4555, 4556, 4580, 4611, 4623

Dowideit, P., Mertens, R., and von Sonntag, C.: Non-hydrolytic decay of formyl chloride into CO and HCl in aqueous solution, J. Am. Chem. Soc., 118, 11,288–11,292, 1996. 4565

Duce, R. A., Arimoto, R., Ray, B. J., Unni, C. K., and Harder, P. J.: Atmospheric trace elements at Enewetak Atoll: 1, Concentrations, sources, and temporal variability, J. Geophys. Res., 88, 5321–5342, 1983. 4552

Finlayson-Pitts, B. J., Livingston, F. E., and Berko, H. N.: Ozone destruction and bromine photochemistry at ground level in the Arctic spring, Nature, 343, 622–625, 1990. 4551

Fortnum, D. H., Battaglia, C. J. Cohen, S. R., and Edwards, J. O.: The kinetics of the oxidation of halide ions by monosubstituted peroxides, J. Am. Chem. Soc., 82, 778–782, 1960. 4574, 4592

Gabriel, R., von Glasow, R., Sander, R., Andreae, M. O., and Crutzen, P. J.: Bromide content of sea-salt aerosol particles collected over the Indian Ocean during INDOEX 1999, J. Geophys. Res., 107(D19), 8032, doi:10.1029/2001JD001133, 2002. 4552

Garratt, J. R., The Atmospheric Boundary Layer, Cambridge University Press, Cambridge, 1992. 4577

Graedel, T. E. and Keene, W. C.: Tropospheric budget of reactive chlorine, Global Biogeochem. Cycles, 9, 47–77, 1995. 4570

Gregory, G. L., Bachmeier, A. S., Blake, D. R., Heikes, B. G., Thornton, D. C., Bandy, A. R., Bradshaw, J. D., and Kondo, Y.: Chemical signatures of aged Pacific marine air: Mixed layer and free troposphere as measured during PEM-West A, J. Geophys. Res., 101, 1727–1742, 1996. 4570, 4576, 4611, 4612

Hedgecock, I. M., Pirrone, N., Sprovieri, F., and Pesenti, E.: Reactive gaseous mercury in the marine boundary layer: modelling and experimental evidence of its formation in the Mediterranean region, Atmos. Environ., 37(S1), 41–49, 2003. 4551

Heikes, B., Lee, M., Jacob, D., Talbot, R., Bradshaw, J., Singh, H., Blake, D., Anderson, B., Fuelberg, H., and Thompson, A. M.: Ozone, hydroperoxides, oxides of nitrogen, and hydrocarbon budgets in the marine boundary layer over the South Atlantic, J. Geophys. Res., 101, 24,221–24,234, 1996. 4554, 4555, 4556, 4557, 4576, 4580, 4611, 4612, 4613, 4623

Hindmarsh, A. C.: ODEPACK, A systematized collection of ode solvers, in Scientific Computing, (Eds.) Stepleman, R. S. et al., pp. 55–64, North-Holland, Amsterdam, 1983. 4576

Hirokawa, J., Onaka, J., Kajii, Y., and Akimoto, H.: Heterogeneous processes involving sodium

halide particles and ozone: Molecular bromine release in the marine boundary layer in the absence of nitrogen oxides, Geophys. Res. Lett., 25, 2449–2452, 1998. 4551

Impey, G. A., Shepson, P. B., Hastie, D. R., and Barrie, L. A.: Measurement technique for the determination of photolyzable chlorine and bromine in the atmosphere, J. Geophys. Res., 102, 15,999–16,004, 1997. 4567

Ingham, T., Bauer, D., Sander, R., Crutzen, P. J., and Crowley, J. N.: Kinetics and products of the reactions BrO + DMS and Br + DMS at 298 K, J. Phys. Chem. A, 103, 7199–7209, 1999. 4553, 4594

James, J. D., Harrison, R. M., Savage, N. H., Allen, A. G., Grenfell, J. L., Allan, B. J., Plane, J. M. C., Hewitt, C. N., Davison, B., and Robertson, L.: Quasi-Lagrangian investigation into dimethyl sulfide oxidation in maritime air using a combination of measurements and model, J. Geophys. Res., 105, 26,379–26,392, 2000. 4551, 4552

Jenkin, M. E., Saunders, S. M., and Pilling, M. J.: The tropospheric degradation of volatile organic compounds: a protocol for mechanism development, Atmos. Environ., 31, 81–104, 1997. 4557, 4572, 4573, 4574, 4587

Johnson, J. E., Gammon, R. H., Larsen, J., Bates, T. S., Oltmans, S. J., and Farmer, J. C.: Ozone in the marine boundary layer over the Pacific and Indian Oceans: Latitudinal gradients and diurnal cycles, J. Geophys. Res., 95, 11,847–11,856, 1990. 4576

Junkermann, W. and Stockwell, W. R.: On the budget of photooxidants in the marine boundary layer of the tropical South Atlantic, J. Geophys. Res., 104, 8039–8046, 1999. 4581

Kaiser, E. W. and Wallington, T. J.: FTIR product study of the Cl-initiated oxidation of CH_3Cl: Evidence for HCl elimination from the chloromethoxy radical, J. Phys. Chem., 98, 5679–5685, 1994. 4565

Knipping, E. M., Lakin, M. J., Foster, K. L., Jungwirth, P., Tobias, D. J., Gerber, R. B., Dabdub, D., and Finlayson-Pitts, B. J.: Experiments and simulations of ion-enhanced interfacial chemistry on aqueous NaCl aerosols, Science, 288, 301–306, 2000. 4551

Kondo, Y., Koike, M., Kawakami, S., Singh, H. B., Nakajima, H., Gregory, G. L., Blake, D. R., Sachse, G. W., Merrill, J. T., and Newell, R. E.: Profiles and partitioning of reactive nitrogen over the Pacific Ocean in winter and early spring, J. Geophys. Res., 102, 28,405–28,424, 1997. 4612

Koppmann, R., Bauer, R., Johnen, F. J., Plass, C., and Rudolph, J.: The distribution of light nonmethane hydrocarbons over the mid-Atlantic: Results of the Polarstern cruise ANT VII/1, J. Atmos. Chem., 15, 215–234, 1992. 4554, 4555, 4591, 4611

Kritz, M. A. and Rancher, J.: Circulation of Na, Cl, and Br in the tropical marine atmosphere, J. Geophys. Res., 85, 1633–1639, 1980. 4582

Kwok, E. S. C. and Atkinson, R.: Estimation of hydroxyl radical reaction rate constants for gas-phase organic compounds using a structure-reactivity relationship: An update, Atmos. Environ., 29, 1685–1695, 1995. 4572, 4587

Kylling, A., 'Phodis, a program for calculation of photodissociation rates in the Earth's atmosphere', available by anonymous ftp to ftp.nilu.no, cd pub/phodis, 1995. 4576

Kylling, A., Stamnes, K., and Tsay, S.-C.: A reliable and efficient two-stream algorithm for spherical radiative transfer: Documentation of accuracy in realistic layered media, J. Atmos. Chem., 21, 115–150, 1995. 4576

Lamontagne, R. A., Swinnerton, J. W., and Linnenbom, V. J.: C_1-C_4 hydrocarbons in the North and South Pacific, Tellus, 26, 71–77, 1974. 4555, 4623

Leser, H., Hönninger, G., and Platt, U.: MAX-DOAS measurements of BrO and NO_2 in the marine boundary layer, Geophys. Res. Lett., 30(10), 1537, doi:10.1029/2002GL015811, 2003. 4552

Levy, H., II, Mahlman, J. D., Moxim, W. J., and Liu, S. C.: Tropospheric ozone: The role of transport, J. Geophys. Res., 90, 3753–3772, 1985. 4577

Lewis, A. C., McQuaid, J. B., Carslaw, N., and Pilling, M. J.: Diurnal cycles of short-lived tropospheric alkenes at a north Atlantic coastal site, Atmos. Environ., 33, 2417–2422, 1999. 4554, 4611

Lewis, A. C., Carpenter, L. J., and Pilling, M. J.: Nonmethane hydrocarbons in Southern Ocean boundary layer air, J. Geophys. Res., 106, 4987–4994, 2001. 4554, 4556, 4611

Libuda, H. G.: Spektroskopische und kinetische Untersuchungen an halogenierten Carbonylverbindungen von atmosphärischem Interesse, Ph-D Thesis, University of Wuppertal, Germany, 1992. 4564, 4573, 4624

Libuda, H. G., Zabel, F., Fink, E. H., and Becker, K. H.: Formyl chloride: UV absorption cross sections and rate constants for the reactions with Cl and OH, J. Phys. Chem., 94, 5860–5865, 1990. 4565

Lightfoot, P. D., Cox, R. A., Crowley, J. N., Destriau, M., Hayman, G. D., Jenkin, M. E., Moortgat, G. K., and Zabel, F.: Organic peroxy radicals: kinetics, spectroscopy and tropospheric chemistry, Atmos. Environ., 26A, 1805–1961, 1992. 4571

Lind, J A., Lazrus, A. L., and Kok, G. L.: Aqueous phase oxidation of sulfur(IV) by hydrogen peroxide, methylhydroperoxide, and peroxyacetic acid, J. Geophys. Res., 92, 4171–4177,

Title Page

Abstract | Introduction

Conclusions | References

Tables | Figures

◄ | ►►

◄ | ►

Back | Close

Full Screen / Esc

Print Version

Interactive Discussion

1987. 4574

Madronich, S. and Calvert, J. G.: Permutation reactions of organic peroxy radicals in the tropo-sphere, J. Geophys. Res., 95, 5697–5715, 1990. 4571

McConnell, J. C., Henderson, G. S., Barrie, L., Bottenheim, J., Niki, H., Langford, C. H., and Templeton, E. M. J.: Photochemical bromine production implicated in Arctic boundary-layer ozone depletion, Nature, 355, 150–152, 1992. 4553, 4588

Mozurkewich, M.: Mechanisms for the release of halogens from sea-salt particles by free radi-cal reactions, J. Geophys. Res., 100, 14,199–14,207, 1995. 4551

Nagao, I., Matsumoto, K., and Tanaka, H.: Sunrise ozone destruction found in the sub-tropical marine boundary layer, Geophys. Res. Lett., 26, 3377–3380, 1999. 4551

Nakano, Y., Goto, M., Hashimoto, S., Kawasaki, M., and Wallington, T.: Cavity ring-down spec-troscopic study of the reactions of Br atoms and BrO radicals with dimethyl sulfide, J. Phys. Chem. A, 105, 11,045–11,050, 2001. 4594

Nielsen, O. J., Munk, J., Locke, G., and Wallington, T. J.: Ultraviolet absorption spectra and kinetics of the self-reaction of CH_2Br and CH_2BrO_2 radicals in the gas phase at 298 K, J. Phys. Chem., 95, 8714–8719, 1991. 4562

Oltmans, S. J. and Levy, H., II: Surface ozone measurements from a global network, Atmos. Environ., 28, 9–24, 1994. 4576

Orlando, J. J., Tyndall, G. S., and Wallington, T. J.: Atmospheric oxidation of CH_3Br: Chemistry of the CH_2BrO radical, J. Phys. Chem., 100, 7026–7033, 1996. 4562, 4563, 4565

Orlando, J. J., Tyndall, G. S., Bilde, M., Ferronato, C., Wallington, T. J., Vereecken, L., and Peeters, J.: Laboratory and theoretical study of the oxy radicals in the OH- and Cl-initiated oxidation of ethene, J. Phys. Chem. A, 102, 8116–8123, 1998. 4562

Orlando, J. J., Tyndall, G. S., Fracheboud, J.-M., Estupiñan, E. G., Haberkorn, S., and Zimmer, A.: The rate and mechanism of the gas-phase oxidation of hydroxyacetone, Atmos. Environ., 33, 1621–1629, 1999. 4624

Pandis, S. N. and Seinfeld, J. H.: Sensitivity analysis of a chemical mechanism for aqueous-phase atmospheric chemistry, J. Geophys. Res., 94, 1105–1126, 1989. 4574

Penkett, S. A., Jones, B. M. R., Rycroft, M. J., and Simmons, D. A.: An interhemispheric comparison of the concentrations of bromine compounds in the atmosphere, Nature, 318, 550–553, 1985. 4576

Plass, C., Koppmann, R., and Rudolph, J., Light hydrocarbons in the surface water of the Mid-Atlantic, J. Atmos. Chem., 15, 235–251, 1992. 4555

Photochemistry of VOCs and halogens in the MBL

K. Toyota et al.

Title Page

Abstract	Introduction
Conclusions	References
Tables	Figures

◄ | ►

◄ | ►

Back | Close

Full Screen / Esc

Print Version

Interactive Discussion

Plass-Dülmer, C., Khedim, A., Koppmann, R., Johnen, F. J., Rudolph, J., and Kuosa, H.: Emissions of light non-methane hydrocarbons from the Atlantic into the atmosphere, Global Biogeochem. Cycles, 7, 211–228, 1993. 4554, 4555, 4556, 4557, 4576, 4580, 4584, 4612, 4613, 4623

Porter, J. N. and Clarke, A. D.: Aerosol size distribution models based on in situ measurements, J. Geophys. Res., 102, 6035–6045, 1997. 4575

Pszenny, A. A. P., Prinn, R. G., Kleiman, G., Shi, X., and Bates, T. S.: Nonmethane hydrocarbons in surface waters, their sea-air fluxes and impact on OH in the marine boundary layer during the First Aerosol Characterization Experiment (ACE 1), J. Geophys. Res., 104, 21,785–21,801, 1999. 4580

Quinn, P. K., Bates, T. S., Johnson, J. E., Covert, D. S., and Charlson, R. J.: Interactions between the sulfur and reduced nitrogen cycles over the central Pacific Ocean, J. Geophys. Res., 95, 16,405–16,416, 1990. 4612

Rahn, K. A., Borys, R. D., and Duce, R. A.: Tropospheric halogen gases: Inorganic and organic components, Science, 192, 549–550, 1976. 4552, 4582

Ramacher, B., Orlando, J. J., and Tyndall G. S.: Temperature-dependent rate coefficient measurements for the reaction of bromine atoms with a series of aldehydes, Int. J. Chem. Kinet., 32, 460–465, 2000. 4559, 4584

Ramacher, B., Orlando, J. J., and Tyndall G. S.: Temperature-dependent rate coefficient measurements for the reaction of bromine atoms with trichloroethene, ethene, acetylene, and tetrachloroethene in air, Int. J. Chem. Kinet., 33, 198–211, 2001. 4560, 4569, 4591

Rancher, J. and Kritz, M. A.: Diurnal fluctuations of Br and I in the tropical marine atmosphere, J. Geophys. Res., 85, 5581–5587, 1980. 4552, 4582

Ratte, M., Plass-Dülmer, C., Koppmann, R., Rudolph, J., and Denga, J.: Production mechanism of C2-C4 hydrocarbons in seawater: Field measurements and experiments, Global Biogeochem. Cycles, 7, 369–378, 1993. 4554, 4555, 4577

Ratte, M., Bujok, O., Spitzy, A., and R., Rudolph, J.: Photochemical alkene formation in seawater from dissolved organic carbon: Results from laboratory experiments, J. Geophys. Res., 103, 5707–5717, 1998. 4555, 4577

Rudolph, J., Koppmann, R., and Plass-Dülmer, Ch.: The budgets of ethane and tetrachloroethene: Is there evidence for an impact of reactions with chlorine atoms in the troposphere?, Atmos. Environ., 30, 1887–1894, 1996. 4594

Rudolph, J., Ramacher, B., Plass-Dülmer, C., Müller, K.-P., and Koppmann, R.: The indirect

determination of chlorine atom concentration in the troposphere from changes in the patterns of non-methane hydrocarbons, Tellus, 49B, 592–601, 1997. 4594

Ruggaber, A., Dlugi, R., Bott, A., Forkel, R., Herrmann, H., and Jacobi, H.-W.: Modelling of radiation quantities and photolysis frequencies in the aqueous phase in the troposphere, Atmos. Environ., 31, 3137-3150, 1997. 4576

Russell, J. J., Seetula, J. A., and Gutman, D.: Kinetics and thermochemistry of methyl, ethyl, and isopropyl. Study of the equilibrium R + HBr $\rightleftharpoons$ R-H + Br, J. Am. Chem. Soc., 110, 3092–3099, 1988. 4560

Saito, T., Yokouchi, Y., and Kawamura, K.: Distributions of C_2–C_6 hydrocarbons over the western North Pacific and eastern Indian Ocean, Atmos. Environ., 34, 4373–4381, 2000. 4554

Sander, R. and Crutzen, P. J.: Model study indicating halogen activation and ozone destruction in polluted air masses transported to the sea, J. Geophys. Res., 101, 9121–9138, 1996. 4551, 4592

Sander, R., Vogt, R., Harris, G. W., and Crutzen, P. J.: Modeling the chemistry of ozone, halogen compounds, and hydrocarbons in the arctic troposphere during spring, Tellus, 49B, 522–532, 1997. 4553, 4591

Sander, R., Rudich, Y., von Glasow, R., and Crutzen, P. J.: The role of $BrNO_3$ in marine tropospheric chemistry: A model study, Geophys. Res. Lett., 26, 2857–2860, 1999. 4551, 4553, 4581, 4594

Saunders, S. M., Jenkin, M. E., Derwent, R. G., and Pilling, M. J.: Protocol for the development of the Master Chemical Mechanism, MCM v3 (Part A): tropospheric degradation of non-aromatic volatile organic compounds, Atmos. Chem. Phys., 3, 161–180, 2003. 4557, 4571, 4572, 4574, 4587

Sehested, J., Nielsen, O. J., and Wallington, T. J.: Absolute rate constants for the reaction of NO with a series of peroxy radicals in the gas phase at 295 K, Chem. Phys. Lett., 213, 457–464, 1993. 4562

Shepson, P. B., Sirju, A.-P., Hopper, J. F., Barrie, L. A., Young, V., Niki, H., and Dryfhout, H.: Sources of sinks of carbonyl compounds in the Arctic Ocean boundary layer: Polar Ice Floe Experiment, J. Geophys. Res., 101, 21,081-21,089, 1996. 4553

Singh, H. B., Gregory, G. L., Anderson, B., Browell, E., Sachse, G. W., Davis, D. D., Crawford, J., Bradshaw, J. D., Talbot, R., Blake, D. R., Thornton, D., Newell, R., and Merrill, J.: Low ozone in the marine boundary layer of the tropical Pacific Ocean: Photochemical loss, chlorine atoms, and entrainment, J. Geophys. Res., 101, 1907–1917, 1996a. 4594

Photochemistry of VOCs and halogens in the MBL

K. Toyota et al.

Title Page

Abstract	Introduction
Conclusions	References
Tables	Figures

◄	►
◄	►
Back	Close

Full Screen / Esc

Print Version

Interactive Discussion

Singh, H. B., Thakur, A. N., Chen, Y. E., and Kanakidou, M.: Tetrachloroethylene as an indicator of low Cl atom concentrations in the troposphere, Geophys. Res. Lett., 23, 1529–1532, 1996b. 4594

Singh, H., Chen, Y., Staudt, A., Jacob, D., Blake, D., Heikes, B., and Snow, J.: Evidence from the Pacific troposphere for large global sources of oxygenated organic compounds, Nature, 410, 1078–1081, 2001. 4554, 4555, 4559, 4576, 4580, 4581, 4583, 4592, 4597, 4611, 4612

Sumner, A. L. and Shepson, P. B.: Snowpack production of formaldehyde and its effect on the Arctic troposphere, Nature, 398, 230–233, 1999. 4553

Thompson, A. M., Johnson, J. E., Torres, A. L., Bates, T. S., Kelly, K. C., Atlas, E., Greenberg, J. P., Donahue, N. M., Yvon, S. A., Saltzman, E. S., Heikes, B. G., Mosher, B. W., Shashkov, A. A., and Yegorov, V. I.: Ozone observations and a model of marine boundary layer photochemistry during SAGA 3, J. Geophys. Res., 98, 16,955-16,968, 1993. 4557, 4576, 4579, 4612, 4613, 4623

Toyota, K., Takahashi, M., and Akimoto, H.: Modeling multi-phase halogen chemistry in the marine boundary layer with size-segregated aerosol module: Implications for quasi-size-dependent approach, Geophys. Res. Lett., 28, 2899–2902, 2001. 4551, 4553, 4554, 4575, 4581, 4594

Tyndall, G. S., Wallington, T. J., Hurley, M. D., and Schneider, W. F.: Rate coefficient for the reaction of CH_2OH radicals with Cl_2 and infrared spectra of chloromethanol and dichloromethanol, J. Phys. Chem., 97, 1576–1582, 1993. 4566

Tyndall, G. S., Orlando, J. J., Wallington, T. J., Dill, M., and Kaiser, E. W: Kinetics and mechanisms of the reactions of chlorine atoms with ethane, propane, and n-butane, Int. J. Chem. Kinet., 29, 43–55, 1997. 4559

Villenave, E. and Lesclaux, R.: The UV absorption spectra of CH_2Br and CH_2BrO_2 and the reaction kinetics of CH_2BrO_2 with itself and with HO_2 at 298 K, Chem. Phys. Lett., 236, 376–384, 1995. 4562, 4571

Villenave, E. and Lesclaux, R.: Kinetics of the cross reactions of CH_3O_2 and $C_2H_5O_2$ radicals with selected peroxy radicals, J. Phys. Chem., 100, 14,372–14,382, 1996. 4571

Villenave, E., Moisan, S., and Lesclaux, R.: Kinetic study of the self-reactions of the $BrCH_2CH_2O_2$ and $BrCH(CH_3)CH(CH_3)O_2$ radicals between 275 and 373 K, J. Phys. Chem. A, 107, 2470–2477, 2003. 4561, 4571

Vogt, R., Crutzen, P. J., and Sander, R.: A mechanism for halogen release from sea-salt aerosol in the remote marine boundary layer, Nature, 383, 327–330, 1996. 4551, 4553, 4592

Photochemistry of VOCs and halogens in the MBL

K. Toyota et al.

Title Page

Abstract	Introduction
Conclusions	References
Tables	Figures

◀ | ▶

◀ | ▶

Back | Close

Full Screen / Esc

Print Version

Interactive Discussion

© EGU 2003

Vogt, R., Sander, R., von Glasow, R., and Crutzen, P. J.: Iodine chemistry and its role in halogen activation and ozone loss in the marine boundary layer: A model study, J. Atmos. Chem., 32, 375–395, 1999. 4551

von Glasow, R., Sander, R., Bott, A., and Crutzen, P. J.: Modeling halogen chemistry in the marine boundary layer, 1. Could-free MBL, J. Geophys. Res., 107(D17), 4341, doi:10.1029/2001JD000942, 2002a. 4551, 4553, 4592

von Glasow, R., Sander, R., Bott, A., and Crutzen, P. J.: Modeling halogen chemistry in the marine boundary layer, 2. Interactions with sulfur and the cloud-covered MBL, J. Geophys. Res., 107(D17), 4323, doi:10.1029/2001JD000943, 2002b. 4551

Wagner, V., von Glasow, R., Fischer, H., and Crutzen, P. J.: Are CH_2O measurements in the marine boundary layer suitable for testing the current understanding of CH_4 photooxidation?: A model study, J. Geophys. Res., 107(D3), doi:10.1029/2001JD000722, 2002. 4553

Wallington, T. J., Skewes, L. M., Siegl, W. O., and Japar, S. M.: A relative rate study of the reaction of bromine atoms with a variety of organic compounds at 295 K, Int. J. Chem. Kinet., 21, 1069–1076, 1989. 4557, 4566

Wallington, T. J., Hurley, M. D., and Schneider, W. F.: Atmospheric chemistry of CH_3Cl: mechanistic study of the reaction of CH_2ClO_2 radicals with HO_2, Chem. Phys. Lett., 251, 164–173, 1996. 4565, 4589

Weller, R., Lorenzen-Schmidt, H., and Schrems, O.: FTIR studies on the photooxidation mechanisms of CH_3Cl, CH_3Br, $CHBr_3$ and CF_3Br, Ber. Bunsenges. Phys. Chem., 96, 409–413, 1992. 4562, 4563, 4565

Wingenter, O. W., Kubo, M. K., Blake, N. J., Smith, T. W., Jr., Blake, D. R., and Rowland, F. S.: Hydrocarbon and halocarbon measurements as photochemical and dynamical indicators of atmospheric hydroxyl, atomic chlorine, and vertical mixing obtained during Lagrangian flights, J. Geophys. Res., 101, 4331–4340, 1996. 4594

Wingenter, O. W., Blake, D. R., Blake, N. J., Sive, B. C., Rowland, F. S., Atlas, E., and Flocke, F.: Tropospheric hydroxyl and atomic chlorine concentrations, and mixing timescales determined from hydrocarbon and halocarbon measurements made over the Southern Ocean, J. Geophys. Res., 104, 21,819–21,828, 1999. 4594

Wisthaler, A., Hansel, A., Dickerson, R. R., and Crutzen, P. J.: Organic trace gas measurements by PTR-MS during INDOEX 1999, J. Geophys. Res., 107(D19), 8024, doi:10.1029/2001JD000576, 2002. 4576, 4581, 4583, 4592, 4611, 4612

Yarwood, G., Peng, N., and Niki, H.: FTIR study of the mechanism of the Cl and Br atom

Photochemistry of VOCs and halogens in the MBL

K. Toyota et al.

Title Page

Abstract	Introduction
Conclusions	References
Tables	Figures

◄ | ►

◄ | ►

Back | Close

Full Screen / Esc

Print Version

Interactive Discussion

initiated oxidation of acetylene, J. Phys. Chem., 95, 7330–7337, 1991. 4569, 4570, 4591

Yarwood, G., Peng, N., and Niki, H.: FTIR spectroscopic study of the Cl- and Br-atom initiated oxidation of ethene, Int. J. Chem. Kinet., 24, 369–383, 1992. 4557, 4560, 4561, 4562, 4571

Yokouchi, Y., Mukai, H., Yamamoto, H., Otsuki, A., Saitoh, C., and Nojiri, Y.: Distribution of methyl iodide, ethyl iodide, bromoform, and dibromomethane over the ocean (east and south-east Asian seas and the western Pacific), J. Geophys. Res., 102, 8805-8809, 1997. 4576

Yokouchi, Y., Li, H.-J., Machida, T., Aoki, S., and Akimoto, H.: Isoprene in the marine boundary layer (Southeast Asian Sea, eastern Indian Ocean, and Southern Ocean): Comparison with dimethyl sulfide and bromoform, J. Geophys. Res., 104, 8067–8076, 1999. 4580

Zafiriou, O. C. and McFarland, M.: Nitric oxide from nitrite photolysis in the central equatorial Pacific, J. Geophys. Res., 86, 3173–3182, 1981. 4577, 4612

Zhou, X. and Mopper, K.: Photochemical production of low-molecular-weight carbonyl compounds in seawater and surface microlayer and their air-sea exchange, Mar. Chem., 56, 201–213, 1997. 4554, 4555, 4556, 4577

Zhu, T., Yarwood, G., Chen, J., and Niki, H.: FTIR study of the Cl + C$_2$H$_2$ reaction: Formation of cis- and trans-CHCl=CH radicals, J. Phys. Chem., 98, 5065–5067, 1994. 4569

Table 1. Mixing ratios of ethene (C_2H_4), propene (C_3H_6), and acetaldehyde (CH_3CHO) in the marine boundary layer with clean air masses reported in the recent literature

Species	Mixing Ratio[a]	Sampling Location	Sampling Dates	Ref.
C_2H_4	58 ± 26	mid-Atlantic, 0° to 45°N	Mar./Apr. 1987	(1)
	45 ± 35	mid-Atlantic, 0° to 45°N	Sep./Oct. 1988	(1)
	25 ± 18	mid-Atlantic, 0° to 30°S	Mar./Apr. 1987	(1)
	22 ± 9	mid-Atlantic, 0° to 30°S	Sep./Oct. 1988	(1)
	$\sim 50^{b}$	central Pacific, 15°S to 20°N and 140° to 170°W	Feb,/Mar. 1990	(2)
	19–30	northern Pacific, 0° to 40°N and 115° to 180°E, north of ITCZ	Sep./Oct. 1991	(3)
	11–24	northern Pacific, 0° to 40°N and 115° to 180°E, south of ITCZ	Sep./Oct. 1991	(3)
	5–21	South Atlantic and western Indian Oceans, 0° to 35.5°S	Sep./Oct. 1992	(4)
	21.0^{c}	Mace Head, 53.3°N 9.9°W	Apr./May 1997	(5, 6)
	9.3^{c}	Cape Grim, 40.7°S 144.7°E	Jan./Feb. 1999	(6)
C_3H_6	$\sim 30^{b}$	central Pacific, 15°S to 20°N and 140° to 170°W	Feb./Mar. 1990	(2)
	9.0–21.5	northern Pacific, 0° to 40°N and 115° to 180°E, north of ITCZ^{d}	Sep./Oct. 1991	(3)
	2–6	South Atlantic and western Indian Oceans, 0° to 35.5°S	Sep./Oct. 1992	(4)
	25.1^{c}	Mace Head, 53.3°N 9.9°W	Apr./May 1997	(5, 6)
	5.2^{c}	Cape Grim, 40.7°S 144.7°E	Jan./Feb. 1999	(6)

Table continued ....

ACPD

3, 4549–4632, 2003

Photochemistry of VOCs and halogens in the MBL

K. Toyota et al.

Title Page

Abstract | Introduction

Conclusions | References

Tables | Figures

◄◄ | ►►

◄ | ►

Back | Close

Full Screen / Esc

Print Version

Interactive Discussion

Table 1. Continued ....

Species	Mixing Ratio[a]	Sampling Location	Sampling Dates	Ref.
CH_3CHO	~80[e]	tropical Pacific, 0° to 30°S and 165°E to 100°W	Mar./Apr. 1999	(7)
	~110[e]	tropical Pacific, 0° to 30°N and 170° to 120°W	Mar./Apr. 1999	(7)
	212±29	equatorial Indian Ocean[f]	Mar. 1999	(8)
	178±30	equatorial Indian Ocean[g]	Mar. 1999	(8)

References: 1, Koppmann et al. (1992); 2, Donahue and Prinn (1993); 3, Gregory et al. (1996); 4, Heikes et al. (1996); 5, Lewis et al. (1999); 6, Lewis et al. (2001); 7, Singh et al. (2001); 8, Wisthaler et al. (2002).

Notes:
[a] Unit: pmol/mol;
[b] Median values;
[c] Average mixing ratios during 11:00-13:00 local time in the clean oceanic air as screened by backward trajectory calculations;
[d] No data was reported for C_3H_6 south of ITCZ;
[e] Mean values;
[f] Northern Hemisphere maritime equatorial air masses;
[g] Southern Hemisphere maritime equatorial air masses

Table 2. Influxes of chemical species that enter in the MBL from the free troposphere or from the ocean

Species	Influx[a]	Reference
Entrainment from the Free Troposphere		
NO_y	1.5×10^9	Estimated[b]
Emissions from the Ocean		
DMS	2×10^9	Quinn et al. (1990)
NO	7×10^7	Zafiriou and McFarland (1981)
C_2H_4	2.4×10^8	Plass-Dülmer et al. (1993)
	2.7×10^8	Heikes et al. (1996)
	6.15×10^8	Thompson et al. (1993)
	1.8×10^9	Bonsang (1993), base case
	5.4×10^9	Donahue and Prinn (1990)
C_3H_6	9.8×10^7	Plass-Dülmer et al. (1993)
	3.1×10^8	Heikes et al. (1996)
	4.45×10^8	Thompson et al. (1993)
	1.0×10^9	Bonsang (1993), base case
	8.8×10^9	Donahue and Prinn (1990)
CH_3CHO	3.6×10^9	Estimated, base case[c]
	8×10^9	Estimated, higher case[c]

Notes:
[a] Unit: $molecule\,cm^{-2}\,s^{-1}$;
[b] Estimated to yield about 10–20 pmol/mol of NO_x (Gregory et al., 1996; Heikes et al., 1996), where NO_y flux from the free troposphere is assumed to comprise 20% NO_x, 30% PAN, and 50% HNO_3 (Kondo et al., 1997);
[c] Estimated to yield CH_3CHO mixing ratios of about 90 pmol/mol (base case; Singh et al., 2001) or about 200 pmol/mol (higher case; Wisthaler et al., 2002)

Title Page

Abstract | Introduction

Conclusions | References

Tables | Figures

◄◄ | ►►

◄ | ►

Back | Close

Full Screen / Esc

Print Version

Interactive Discussion

Table 3. Overview of model runs

No.	Brief Description
1a	Base run; alkene emission rates taken from Bonsang (1993)
1b	The same as Run 1a but without the oceanic emission of CH_3CHO
1c	The same as Run 1a but with the higher emission rate of CH_3CHO from the ocean
1d	The same as Run 1a but without the oceanic emission of C_2H_4
1e	The same as Run 1a but without the oceanic emission of C_3H_6
1f	The same as Run 1a but with absorption cross sections for brominated hydroperoxides being red-shifted by 50 nm
1g	The same as Run 1a but with reduced γ values (= 8×10^{-4}) for hydrolysis of HCOBr/HCOCl on aerosols
1h	The same as Run 1a but with $[C_2H_2]=200$ pmol/mol
1i	The same as Run 1g but with $[C_2H_2]=200$ pmol/mol
1j	The same as Run 1a but with halogen chemistry being switched off by taking off the atmospheric loading of sea-salt aerosols and by specifying $[CHBr_3]=0$ pmol/mol
2	No alkene emissions from the ocean
3	Alkene emission rates taken from Plass-Dülmer et al. (1993)
4	Alkene emission rates taken from Heikes et al. (1996)
5	Alkene emission rates taken from Thompson et al. (1993)
6	Alkene emission rates taken from Donahue and Prinn (1990)

Table continued ....

Table 3. Continued ....

No.	Brief Description
7a	Similar to Run 2 but with the mixing ratios of C_2H_4, C_3H_6, HCHO, and CH_3CHO being fixed at 0.0, 0.0, 265.6, and 80.2 pmol/mol, respectively
7b	Similar to Run 1a but with the mixing ratios of C_2H_4, C_3H_6, HCHO, and CH_3CHO being fixed at 89.9, 12.6, 301.2, and 94.7 pmol/mol, respectively
7c	The same as Run 7a but with the mixing ratios of HCHO and CH_3CHO being fixed at 301.2 and 94.7 pmol/mol, respectively
7d	The same as Run 7b but with the mixing ratios of HCHO and CH_3CHO being fixed at 265.6 and 80.2 pmol/mol, respectively
8a	Parameter sweep experiment; multiple model runs are performed in which different mixing ratios of CH_3CHO are specified ranging from 0 to 250 pmol/mol with those of HCHO, C_2H_4, and C_3H_6 being fixed at 300, 30, and 15 pmol/mol, respectively
8b	Parameter sweep experiment; multiple model runs are performed in which different mixing ratios of C_2H_4 are specified ranging from 0 to 100 pmol/mol with those of HCHO, CH_3CHO, and C_3H_6 being fixed at 300, 90, and 15 pmol/mol, respectively
8c	Parameter sweep experiment; multiple model runs are performed in which different mixing ratios of C_3H_6 are specified ranging from 0 to 30 pmol/mol with those of HCHO, CH_3CHO, and C_2H_4 being fixed at 300, 90, and 30 pmol/mol, respectively

Table 4. Mixing ratios of C_2H_4, C_3H_6, HCHO, CH_3CHO, CH_3OOH, $CH_3C(O)OOH$ (PAA), total inorganic gaseous bromine (i-Br_x), total brominated organic intermediates in the gas phase formed via Br-initiated degradation of C_2H_4, C_3H_6, and C_2H_2 (o-Br_x), NO_x, and DMS, OH concentrations, Br^- loss from sea-salt aerosols, and net chemical production rates of O_3 (P–L(O_3)) as simulated in Runs 1a–j and 2–6. Daily averaged values on Day 20 are presented

	1a	1b	1c	1d	1e	1f	1g	1h	1i
$C_2H_4{}^{a}$	89.9	83.0	95.0	0.0069^d	88.2	90.0	89.9	90.0	89.9
$C_3H_6{}^{a}$	12.6	11.3	13.4	12.3	0.0	12.6	12.6	12.6	12.6
HCHO^{a}	301.2	260.8	331.2	283.4	285.6	298.8	302.0	301.1	302.0
CH_3CHO^{a}	94.7	11.6	209.9	91.8	83.7	94.2	94.8	94.8	94.9
CH_3OOH^{a}	793.3	824.8	800.8	821.9	814.9	798.9	791.5	793.4	791.4
PAA^{a}	79.8	26.9	140.1	79.8	70.8	80.4	79.7	80.0	79.8
Br^- loss	37.5%	63.9%	21.6%	40.2%	43.0%	38.4%	37.3%	37.2%	37.1%
i-$Br_x{}^{a}$	5.22	14.37	2.17	6.43	8.08	5.95	4.99	5.15	4.90
o-$Br_x{}^{a}$	1.54	5.83	0.51	1.38	0.70	1.10	1.64	1.52	1.62
OH^{b}	9.04	9.49	8.60	9.27	9.16	9.02	9.05	9.04	9.05
$NO_x{}^{a}$	19.5	11.5	23.4	18.2	16.8	18.8	19.7	19.5	19.8
DMS^{a}	74.5	44.6	90.7	69.2	64.7	72.3	75.3	74.9	75.7
P–L(O_3)^{c}	−1.09	−1.79	−0.86	−1.18	−1.28	−1.14	−1.08	−1.09	−1.07

Table continued ...

Table 4. Continued ...

	1j	2	3	4	5	6
$C_2H_4{}^a$	88.3	0.0	11.5	13.0	29.9	329.2
$C_3H_6{}^a$	12.6	0.0	1.2	3.7	5.4	134.3
$HCHO^a$	322.5	265.6	270.3	274.7	280.8	406.7
CH_3CHO^a	97.0	80.2	81.9	84.4	86.6	202.0
CH_3OOH^a	747.2	850.7	842.4	835.1	824.6	733.3
PAA^a	75.7	71.2	71.9	73.7	74.9	156.5
Br^- loss	–	48.1%	46.3%	44.3%	42.5%	21.0%
$i\text{-}Br_x{}^a$	0.00	10.85	9.82	8.66	7.66	1.08
$o\text{-}Br_x{}^a$	0.00	0.00068^e	0.33	0.71	0.97	2.01
OH^b	9.37	9.40	9.35	9.32	9.26	7.34
$NO_x{}^a$	25.1	14.7	15.4	16.3	17.1	25.6
DMS^a	93.0	56.5	59.2	62.4	65.5	108.4
$P\text{--}L(O_3)^c$	–0.71	–1.46	–1.39	–1.32	–1.26	–0.79

Notes:
[a] Unit: pmol/mol;
[b] Unit: 10^5 molecule/cm^3;
[c] Unit: nmol/mol/day, a negative value implies net chemical loss;
[d] Formed via photolysis of acrolein (CH_2=CHCHO), which is a minor product of C_3H_6 degradation;
[e] HCOBr formed via reaction $Br + C_2H_2$

Table 5. Sources and sinks for brominated hydroperoxides, $CH_3CH(OOH)CH_2Br$, $BrCH_2CH_2OOH$, and $BrCH_2OOH$, on Day 20 in Run 1a. Since more than two different mechanisms contribute to the loss of each compound, the relative contribution of each loss mechanism is also given in parenthesis

---

$[CH_3CH(OOH)CH_2Br] = 0.377\,pmol/mol$

– Source –

$CH_3CH(OO)CH_2Br + HO_2$ 　　　　　　　　　　0.512 pmol/mol/day

– Sink –

$CH_3CH(OOH)CH_2Br + h\nu \rightarrow$ 　　　　　　　0.039 pmol/mol/day (7.7%)
　　　$0.86 \times CH_3COCH_2Br + 0.14 \times BrCH_2OO$ + products

$CH_3CH(OOH)CH_2Br + OH \rightarrow CH_3C(OO)CH_2Br + H_2O$ 　0.114 pmol/mol/day (22.2%)

$CH_3CH(OOH)CH_2Br + OH \rightarrow CH_3C(O)CH_2Br + OH + H_2O$ 　0.251 pmol/mol/day (49.0%)

dry deposition 　　　　　　　　　　　　　　　0.108 pmol/mol/day (21.2%)

$[BrCH_2CH_2OOH] = 0.145\,pmol/mol$

– Source –

$BrCH_2CH_2OO + HO_2$ 　　　　　　　　　　　0.147 pmol/mol/day

– Sink –

$BrCH_2CH_2OOH + h\nu \rightarrow BrCH_2CHO + HO_2 + OH$ 　0.015 pmol/mol/day (10.2%)

$BrCH_2CH_2OOH + OH \rightarrow BrCH_2CH_2OO + H_2O$ 　0.043 pmol/mol/day (29.5%)

$BrCH_2CH_2OOH + OH \rightarrow BrCH_2CHO + OH + H_2O$ 　0.047 pmol/mol/day (31.9%)

dry deposition 　　　　　　　　　　　　　　　0.042 pmol/mol/day (28.5%)

Title Page

Abstract | Introduction

Conclusions | References

Tables | Figures

|◄ | ►|

◄ | ►

Back | Close

Full Screen / Esc

Print Version

Interactive Discussion

Table 5. Continued ....

[BrCH$_2$OOH] = 0.373 pmol/mol	
– Source –	
BrCH$_2$OO + HO$_2$	0.353 pmol/mol/day
– Sink –	
BrCH$_2$OOH + $h\nu$ → 0.99 × Br + 0.01 × HCOBr + products	0.037 pmol/mol/day (10.5%)
BrCH$_2$OOH + OH → BrCH$_2$OO + H$_2$O	0.107 pmol/mol/day (30.5%)
BrCH$_2$OOH + OH → HCOBr + OH + H$_2$O	0.101 pmol/mol/day (28.6%)
dry deposition	0.107 pmol/mol/day (30.4%)

Table 6. Sources and sinks for brominated carbonyl compounds, CH_3COCH_2Br, $BrCH_2CHO$, and $HCOBr$, on Day 20 in Run 1a. Since quite a lot of mechanisms contribute to the production/loss of each compound, common mechanisms are lumped together. A relative contribution of each common production/loss mechanism is also given in parenthesis. Mechanisms contributing less than 0.2% of the overall production/loss are disregarded

$[CH_3COCH_2Br] = 0.139\,pmol/mol$	
– Source –	
$CH_3CH(OO)CH_2Br + NO/CH_3OO$	0.248 pmol/mol/day (46.1%)
$CH_3CH(OOH)CH_2Br + OH/h\nu$	0.285 pmol/mol/day (53.0%)
$CH_3CH(OH)CH_2Br + OH$	0.005 pmol/mol/day (0.9%)
– Sink –	
$CH_3COCH_2Br + h\nu \rightarrow 0.625 \times BrCH_2OO$ $+ 0.25 \times BrCH_2C(O)OO + 0.125 \times Br + products$	0.523 pmol/mol/day (97.3%)
$CH_3COCH_2Br + OH \rightarrow CH_3COCHBrOO + H_2O$	0.0034 pmol/mol/day (0.6%)
dry deposition	0.011 pmol/mol/day (2.0%)

Table continued ....

Table 6. Continued ....

[BrCH$_2$CHO] = 0.113 pmol/mol

– Source –

BrCH$_2$CH$_2$OO + NO/CH$_3$OO	0.105 pmol/mol/day (55.8%)
BrCH$_2$CH$_2$OOH + OH/$h\nu$	0.062 pmol/mol/day (32.7%)
BrCH$_2$CH$_2$OH + OH	0.0079 pmol/mol/day (4.2%)
Br + acrolein	0.014 pmol/mol/day (7.2%)

– Sink –

BrCH$_2$CHO + $h\nu$ →	0.104 pmol/mol/day (55.5%)
$\quad$ 0.997 × BrCH$_2$OO + 0.003 × CH$_3$Br + products	
BrCH$_2$CHO + OH → 0.5 × BrCH$_2$C(O)OO	0.037 pmol/mol/day (19.5%)
$\quad$ + 0.25 × (BrCH$_2$OO + Br) + products	
dry/wet deposition	0.047 pmol/mol/day (24.8%)

[HCOBr] = 0.012 pmol/mol

– Source –

BrCH$_2$OO + HO$_2$	0.039 pmol/mol/day (27.2%)
BrCH$_2$O + O$_2$	0.00084 pmol/mol/day (0.6%)
BrCH$_2$OOH + OH	0.101 pmol/mol/day (69.8%)
Br + C$_2$H$_2$	0.0035 pmol/mol/day (2.4%)

– Sink –

HCOBr → HBr + CO (on aerosols)	0.134 pmol/mol/day (93.0%)
HCOBr + OH/$h\nu$ → Br + proudcts	0.005 pmol/mol/day (3.5%)
dry/wet deposition	0.005 pmol/mol/day (3.5%)

Title Page

Abstract | Introduction

Conclusions | References

Tables | Figures

|◄ | ►|

◄ | ►

Back | Close

Full Screen / Esc

Print Version

Interactive Discussion

© EGU 2003

Table 7. Total mixing ratios of inorganic gaseous bromine species (i-Br$_x$) in Runs 7a–d. Daily averaged values on Day 20 are presented

	$C_2H_4{}^{a,b}$	$C_3H_6{}^{a,b}$	HCHO^{a,b}	CH$_3$CHO^{a,b}	i-Br$_x{}^a$
7a	0.0	0.0	265.6	80.2	11.15
7b	89.9	12.6	301.2	94.7	5.26
7c	0.0	0.0	301.2	94.7	7.87
7d	89.9	12.6	265.6	80.2	6.75

Notes:
[a] Unit: pmol/mol;
[b] Mixing ratios are fixed at given values

Table 8. Rates of reactive halogen production via reactions of potential importance for triggering autocatalytic halogen release from sea-salt aerosols as simulated in Run 1a[a]. Values averaged over the nighttime (00:00–06:00, 18:00–24:00 local sun time) and over the daytime (06:00–12:00 local sun time) on Day 20 are presented

Reaction(s)	Product	Nighttime	Daytime
$Br^- + HSO_5^-$ [b]	HOBr	1.4×10^{-3}	1.5×10^{-2}
$Cl^- + HSO_5^-$ [b]	HOCl	3.0×10^{-3}	6.7×10^{-2}
$Br_2^- + Br_2^-$ [b]	Br_2	5.4×10^{-4}	3.8×10^{-2}
$Cl_2^- + Cl_2^-$ [b]	Cl_2	2.2×10^{-5}	3.0×10^{-3}
$Br^- + O_3$ [b]	HOBr	1.4×10^{-3}	1.1×10^{-3}
$Br^- + PAA$ [b]	HOBr	4.1×10^{-4}	3.7×10^{-4}
$Cl^- + PAA$ [b]	HOCl	7.6×10^{-4}	7.6×10^{-4}
$Br^- + HNO_4$ [b]	HOBr	9.7×10^{-7}	1.6×10^{-5}
$Cl^- + HNO_4$ [b]	HOCl	2.2×10^{-6}	4.3×10^{-5}
$CHBr_3$ degradation [c]	Br	5.6×10^{-6}	7.7×10^{-3}

Notes:
[a] Unit: pmol(Br)/mol/hour or pmol(Cl)/mol/hour;
[b] Integrated over aerosol size bins except for the largest-size bin, which remains alkaline over the whole simulation time;
[c] The formation of Br atoms via $CHBr_3$ photolysis, OH- and Cl-attacks on $CHBr_3$, and CBr_2O photolysis is accounted for, whereas the formation of HBr via $CHBr_3$ photolysis is not.
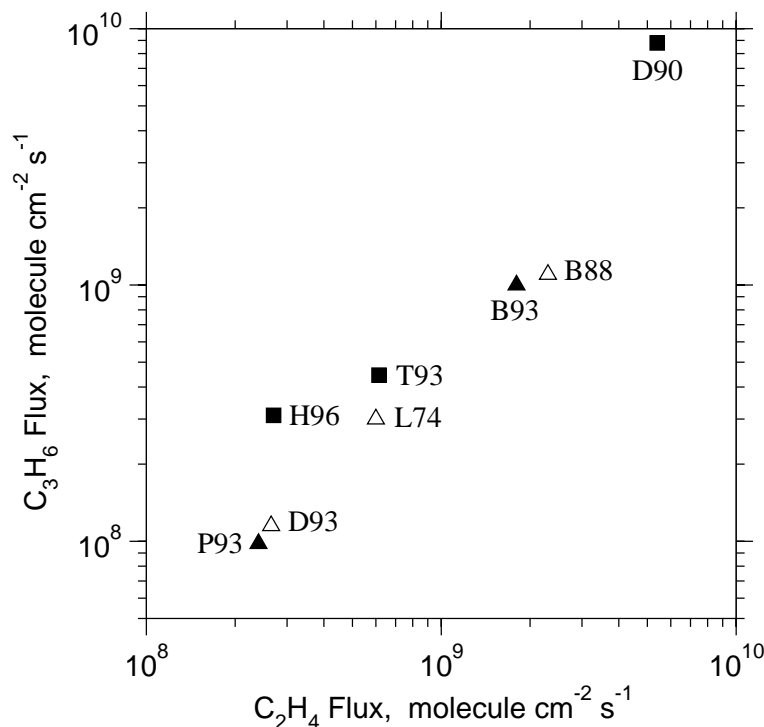
Fig. 1. Estimated sea-to-air fluxes of C_2H_4 and C_3H_6 reported in the literature: P93, Plass-Dülmer et al. (1993); D93, Donahue and Prinn (1993); H96, Heikes et al. (1996), T93, Thompson et al. (1993); B93, Bonsang (1993); D90, Donahue and Prinn (1990); L74 and B88 were calculated by Donahue and Prinn (1990) from the data of Lamontagne et al. (1974) and Bonsang et al. (1988), respectively. Values marked by triangles were estimated based on measured seawater concentrations with a diffusive microlayer approach and those marked by squares based on measured air concentrations with budget analyses using photochemical models. Values with filled marks (P93, H96, T93, B93, and D90) are used in the model runs of the present work.
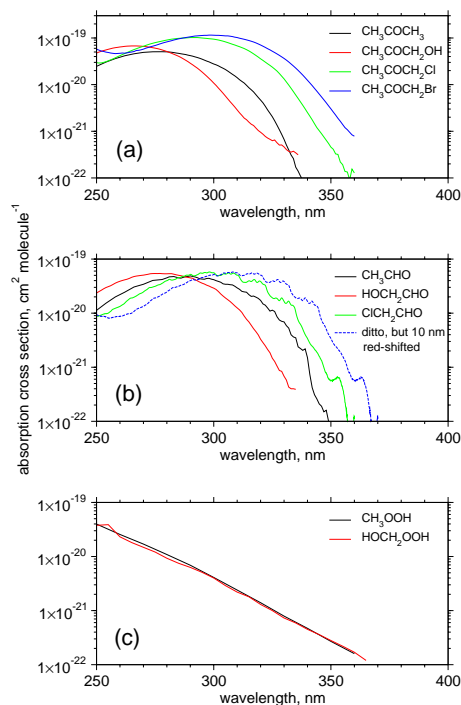
Fig. 2. (a) Experimentally determined absorption cross sections for acetone and its substituted analogues: CH_3COCH_3 (black line; Atkinson et al., 1999), CH_3COCH_2OH (red line; Orlando et al., 1999), CH_3COCH_2Cl and CH_3COCH_2Br (green and blue lines, respectively; Burkholder et al., 2002); **(b)** absorption cross sections for acetaldehyde and its substituted analogues: CH_3CHO (black line; Atkinson et al., 1999), $HOCH_2CHO$ (red line; Bacher et al., 2001), and $ClCH_2CHO$ (green line; Libuda, 1992); absorption cross sections for $BrCH_2CHO$ have not been reported in the literature and are therefore assumed red-shifted by 10 nm relative to those for $ClCH_2CHO$ (blue dashed line); and **(c)** absorption cross sections for methyl hydroperoxide and its OH-substituted analogue: CH_3OOH (black line; Atkinson et al., 1999) and $HOCH_2OOH$ (red line; Bauerle and Moortgat, 1999).
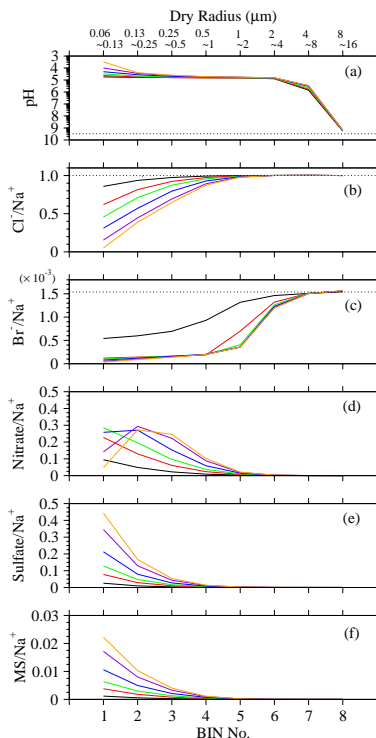
Fig. 3. Simulated temporal evolutions of pH **(a)**, Cl^-/Na^+ molar ratio **(b)**, Br^-/Na^+ molar ratio **(c)**, $(HNO_3 + NO_3^-)/Na^+$ molar ratio **(d)**, $(HSO_4^- + SO_4^{2-})/Na^+$ molar ratio **(e)**, $(CH_3SO_3H + CH_3SO_3^-)/Na^+$ molar ratio **(f)** as a function of particle size of the sea-salt aerosols for Run 1a. Daily averaged values on Days 1 (black lines), 2 (red lines), 3 (green lines), 5 (blue lines), 10 (violet lines), 20 (orange lines) are presented. Dotted lines correspond to values in nascent sea-salt aerosols.
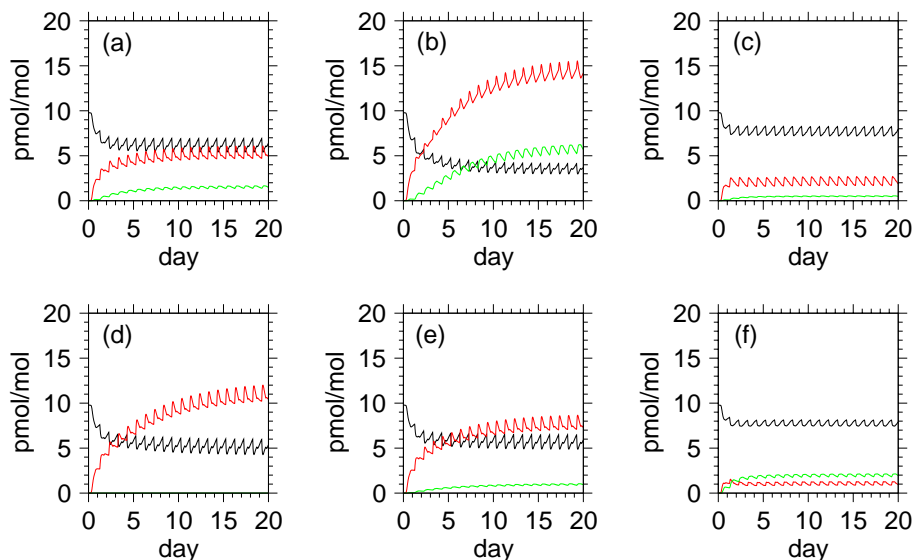
Fig. 4. Impacts of the oceanic emissions of acetaldehyde and alkenes on the simulated mixing ratios of bromine species: **(a)** Run 1a, **(b)** Run 1b, **(c)** Run 1c, **(d)** Run 2, **(e)** Run 5, and **(f)** Run 6. Black lines represent the total mixing ratios of Br^- in sea-salt aerosols, red lines the total mixing ratios of inorganic gaseous bromine species, and green lines the total mixing ratios of organic gaseous bromine species formed via Br-initiated degradation of C_2H_4, C_3H_6, and C_2H_2.
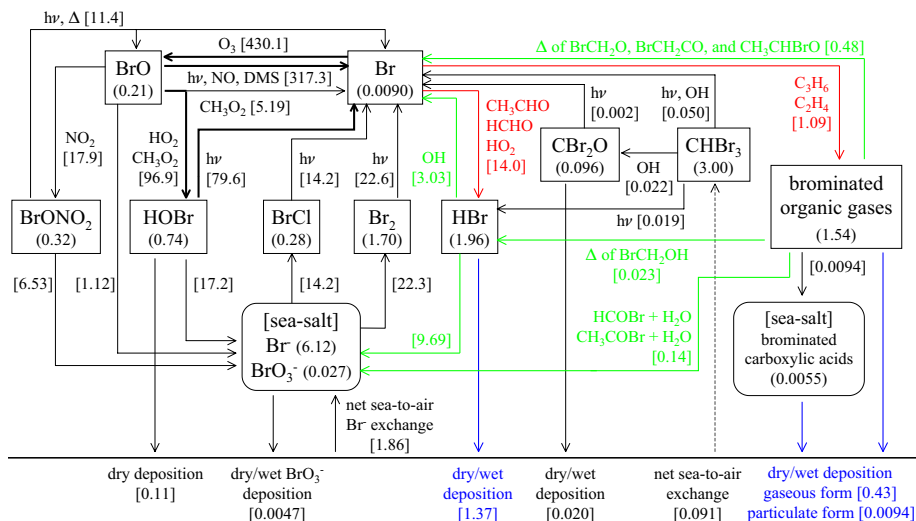
Fig. 5. The material cycle of bromine species as simulated on Day 20 in Run 1a. The numbers in parentheses are daily average mixing ratios in pmol(Br)/mol and those in brackets the rates of either chemical transformation or air-sea mass exchange in pmol(Br)/mol/day. "Δ" represents decomposition via either thermal unimolecular reaction or fragmentation of an excited molecule. Where two or more reactions contribute to the same transformation pathway, only those contributing by more than 2% of the total are listed in order of their relative importance. Small imbalance in mass flow rates apparent for Br_2 is caused by neglecting a contribution from Br_2 formation via self-reaction of BrO. The net sea-to-air exchange rate of $CHBr_3$ is calculated so as to balance with its photochemical loss in the air, since the mixing ratio of this compound is specified rather than simulated in the model.
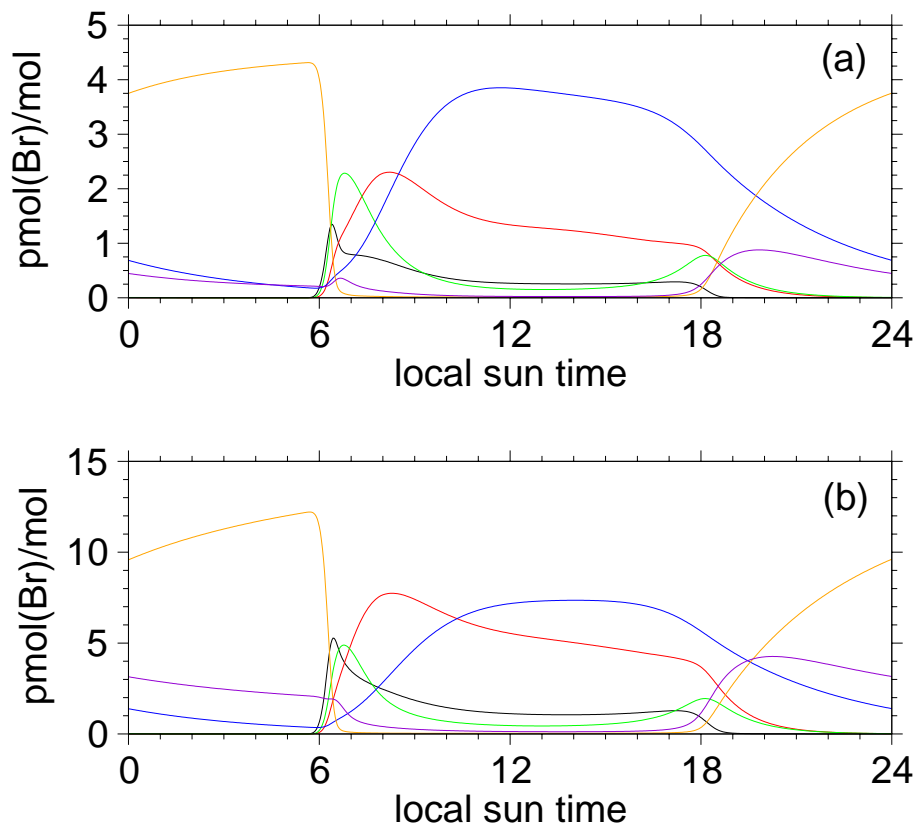
Fig. 6. Diurnal variations in the mixing ratios of major reservoirs of inorganic gaseous bromine species (HBr, blue lines; HOBr, red lines; BrONO$_2$, green lines; BrO, black lines; Br$_2$, orange lines; and BrCl, violet lines) simulated on Day 20 for Runs 1a **(a)** and 1b **(b)**.
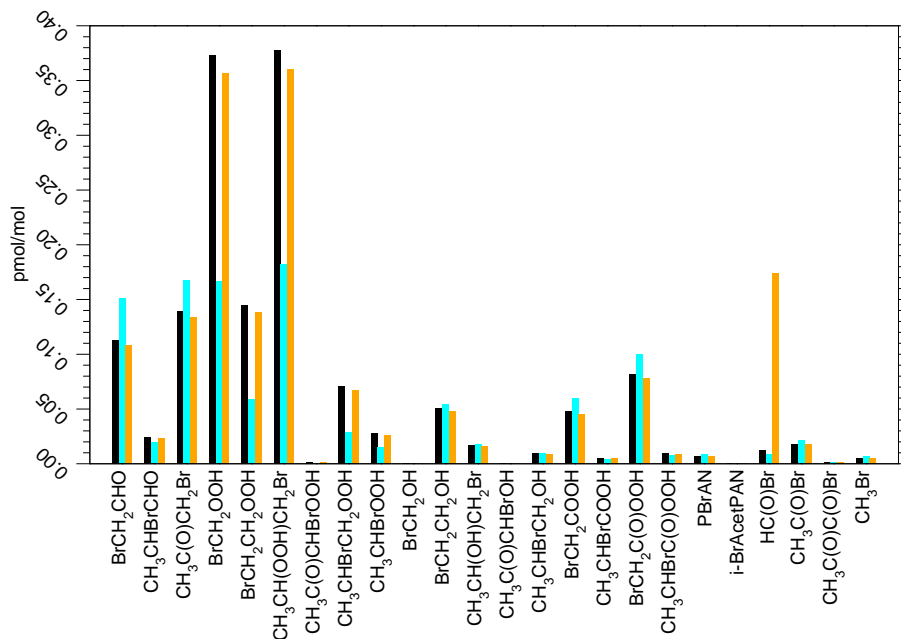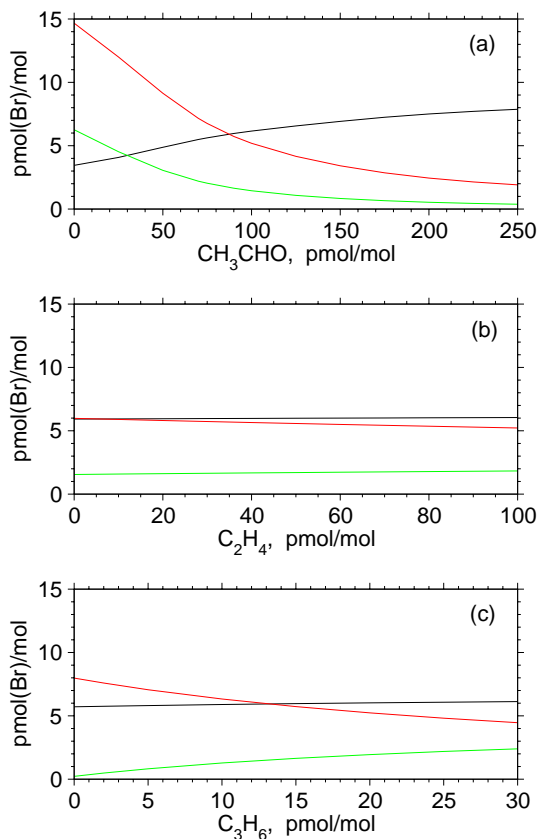
Fig. 7. Mixing ratios of brominated organic intermediates formed via Br-initiated degradation of C_2H_4, C_3H_6, and C_2H_2 in Run 1a (black bars), Run 1f (blue bars), and Run 1g (orange bars). Daily averaged values on Day 20 are presented.

Fig. 8. The total mixing ratios of Br^- in sea-salt aerosols (black lines), those of inorganic gaseous bromine species (red lines), and those of brominated organic intermediates (green lines) obtained on Day 20 in parameter sweep experiments: **(a)** Run 8a, **(b)** Run 8b, and **(c)** Run 8c.
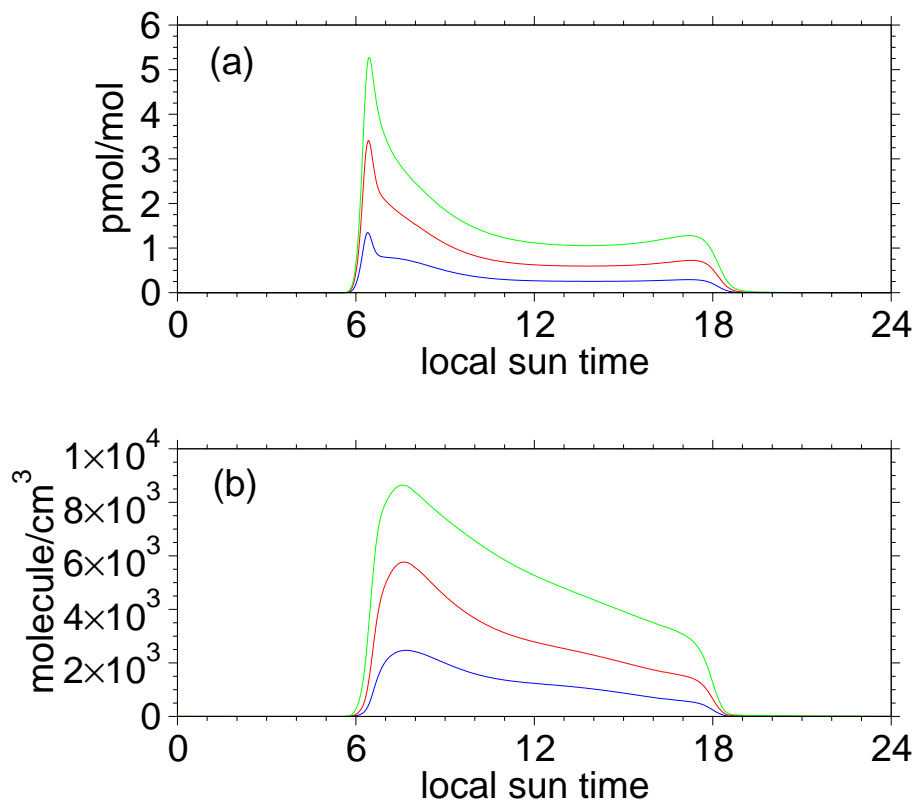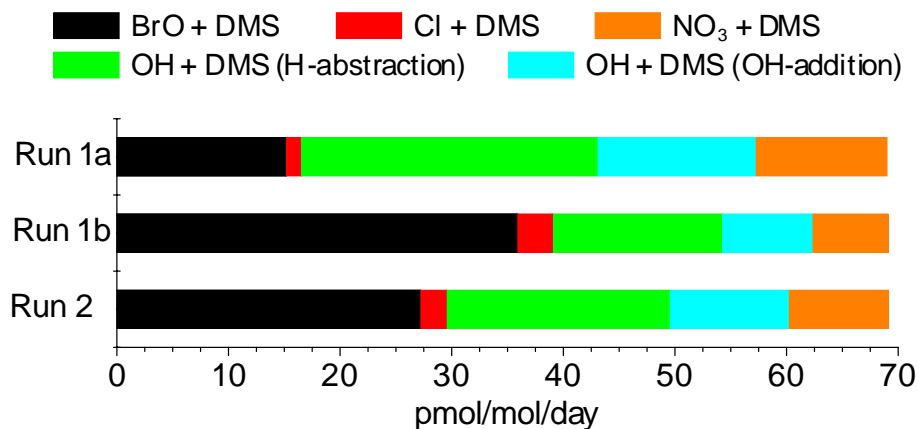
Fig. 9. Diurnal variations in BrO mixing ratios **(a)** and Cl-atom concentrations **(b)** on Day 20 for Runs 1a (blue lines), 1b (green lines), and 2 (red lines).

Fig. 10. DMS oxidation pathways on Day 20 for Runs 1a–b and 2.

© EGU 2003